# Terrestrial Gross Primary Production: Using $NIR_V$ to Scale from Site to Globe

Grayson Badgley[1,2,+,*], Leander D.L. Anderegg[1,3,+], Joseph A. Berry[1], Christopher B. Field[2,4]

1. Department of Global Ecology, Carnegie Institution for Science, Stanford, CA, 94305
2. Department of Earth System Science, Stanford University, Stanford, CA, 94305
3. Department of Integrative Biology, University of California, Berkeley, CA, 94720
4. Woods Institute for the Environment, Stanford University, Stanford, CA, 94305

* badgley@stanford.edu

+ These authors contributed equally

## Abstract

Terrestrial photosynthesis is the largest and one of the most uncertain fluxes in the global carbon cycle. We find that $NIR_V$, a remotely sensed measure of canopy structure, accurately predicts photosynthesis at FLUXNET validation sites at monthly to annual timescales ($R^2 = 0.68$), without the need for difficult to acquire information about environmental factors that constrain photosynthesis at short timescales. Scaling the relationship between GPP and $NIR_V$ from FLUXNET eddy covariance sites, we estimate global annual terrestrial photosynthesis to be 147 Pg C $y^{-1}$ (95% credible interval 131-163 Pg C $y^{-1}$), which falls between bottom-up GPP estimates and the top-down global constraint on GPP from oxygen isotopes. $NIR_V$-derived estimates of GPP are systematically higher than existing bottom-up estimates, especially throughout the mid-latitudes. Progress in improving estimated GPP from $NIR_V$ can come from improved cloud-screening in satellite data and increased resolution of vegetation characteristics, especially photosynthetic pathway.

# 1 Introduction

Terrestrial photosynthesis (or gross primary production (GPP)) is responsible for fixing somewhere between 119 and 169 Pg C $y^{-1}$, making GPP both the largest and most uncertain component of the global carbon cycle (Anav et al., 2015). Carbon fixed by photosynthesis in turn provides the basis for practically all life on land, providing a strong motivation for improving global estimates of GPP. It is especially important to understand how photosynthesis might respond to global environmental change, as minor perturbations in terrestrial productivity have implications for global biodiversity, agriculture, and climate change (Rockström et al., 2009; Running, 2012).

A global network of eddy covariance measurements of land surface $CO_2$ exchange serves as the primary basis for quantifying terrestrial photosynthesis at both the site and global scale (Baldocchi, 2008; Baldocchi et al., 2001). Despite their utility, eddy covariance measurements are limited in both time and space; individual flux sites measure $CO_2$ fluxes over approximately 1 $km^2$ and, in any given year, fewer than 100 sites operate globally (Kumar et al., 2016). Nevertheless, these sparse measurements are the best available data both for studying ecosystem-scale photosynthetic processes at the global scale and for validating terrestrial ecosystem models, which operate globally at resolutions typically much greater than a single kilometer and need to integrate over processes with time constants from a fraction of a second to many years.

In response to the sparseness of photosynthesis observations, a host of semi-empirical upscaling approaches have emerged for translating site-level $CO_2$ fluxes to globally gridded photosynthesis estimates. Upscaling depends on the assumption that functional relationships between driver variables and GPP operate the same way at measured and unmeasured sites. Though many upscaling schemes exist, two approaches are by far the most widely used: machine learning (Beer et al., 2010; Tramontana et al., 2016) and satellite-driven mechanistic models (Running et al., 2004; Ryu et al., 2011). Both approaches integrate some combination of site-level abiotic characteristics, plant traits, and meteorology to estimate photosynthesis, using *in situ* fluxes from eddy covariance installations to calculate scaling factors that allow estimation of photosynthesis beyond tower footprints. Such approaches have been quite successful, allowing for both the investigation of the drivers of global photosynthesis (Jung et al., 2017; Zhao et al., 2010) and more extensive benchmarking of photosynthesis models by expanding the temporal and spatial availability of photosynthesis estimates (Bonan et al., 2011; Williams et al., 2009).

Any upscaling introduces uncertainties into GPP estimates, stemming both from model

formulation and input data. Machine learning approaches, for example, provide the best possible constraint on GPP based on available data, but they functionally operate as black boxes. Such complexity makes it difficult to diagnose the causes and consequences of uncertainty. Upscaling approaches are also limited by the availability of and the uncertainties contained within input datasets (e.g., meteorological data). Combined, these challenges limit the utility of existing upscaling approaches for improving our process-based understanding of photosynthesis and determining the true value of global GPP. Of particular concern is the large and persistent disconnect between upscaled estimates of global GPP and higher estimates derived from top-down isotopic constraints (Welp et al., 2011).

Here, we report a novel approach for estimating global GPP using the near-infrared reflectance of vegetation ($NIR_V$) that takes conceptual root in ideas going back more than 40 years. Even before the widespread use of remote sensing in vegetation analyses, Monteith (1977) observed that the annual increment in biomass growth (net primary production; NPP) can be estimated as the product of the annual absorption of solar radiation and a radiation use efficiency that is relatively constant across species. Several early remote sensing studies built on this idea, documenting the strong correlation between biomass accumulation and the annual integral of the normalized vegetation index (NDVI) (Goward et al., 1985; Tucker et al., 1985). While these approaches for estimating NPP worked well at longer time scales, short-term responses were inconsistent and variable across sites (Running et al., 1988). Progress in improving the performance of NDVI-based productivity models came from a mix of incorporating additional information about vegetation type, meteorology, and physiological stress. As a result, integration approaches gradually transitioned to more physiologically grounded models, which attempt to represent the biochemical processes (e.g., carbon fixation by rubisco) and physiological stress responses (e.g., stomatal closure due to low soil moisture) that control photosynthesis (Field et al., 1995; Myneni et al., 1995; Potter et al., 1993; Running et al., 2004; Sellers et al., 1996). Though inclusion of biochemical and physiological processes made photosynthesis models more robust at shorter timescales, it introduced the vexing problem of needing to independently specify key physiological parameters, such as the maximum rate of carboxylation of rubisco ($V_{Cmax}$). Inconsistencies in model parameterization schemes, in turn, give rise to large divergences in model-based estimates of GPP and belie fundamental uncertainties in our understanding of the controls on photosynthesis at the global scale (Schaefer et al., 2012).

We revisit the early strategies for directly relating integrated satellite measurements to plant productivity. Our approach employs the near-infrared reflectance of vegetation ($NIR_V$), a new

satellite product that approximates the proportion of near-infrared light reflected by vegetation. $NIR_V$ offers several advantages over existing satellite vegetation indices. Namely, $NIR_V$ has a robust physical interpretation, as it relates directly to the number of NIR photons reflected by plants (Badgley et al., 2017). As a result, $NIR_V$ minimizes both the effects soil contamination and variable viewing geometry on satellite-derived spectra. Consequently, $NIR_V$ serves as a comprehensive index of light capture, integrating the influence of leaf area, leaf orientation, and overall canopy structure. We hypothesize that, to the extent plants allocate resources efficiently (Bloom et al., 1985; Field et al., 1995), this integrated measure of investment in light capture should scale with the capacity to fix $CO_2$, providing a strong basis for new, satellite-derived estimates of GPP.

To test this hypothesis, we use the relationship between $NIR_V$ and *in situ* measurements of GPP derived from eddy covariance. We present our results in three parts. First, we validate the $NIR_V$-GPP relationship at the site scale, contrasting the $NIR_V$ approach with other remote sensing, statistical, and physiological models of GPP. Second, we extend the relationship to consider global GPP. Third, we evaluate some of the limitations in the global dataset of $NIR_V$ and discuss options for refining the approach.

# 2 Materials and Methods

## 2.1 Data

We compared $NIR_V$, which is the product of the normalized difference vegetation index (NDVI) and NIR reflectance ($NDVI \cdot NIR$), against monthly and annual GPP fluxes at 105 flux sites contained in the FLUXNET2015 Tier 1 dataset that met quality control requirements and fell within the time frame of the MODIS record (2003-present). We calculated median NDVI and NIR for all daily scenes overlapping a $1km^2$ circle around each fluxsite, using 500 meter, daily red (620-670nm) and near-infrared (NIR, 841-876nm) nadir-adjusted reflectances from MODIS collection MCD43A4.006 hosted on Google Earth Engine for the years spanning 2003 to 2015 (Schaaf et al., 2015). Prior to estimating mean $NIR_V$, gaps in reflectance data of up to seven days were filled using linear interpolation. We calculated the average of all $NIR_V$ observations for each month and compared them with monthly estimates of GPP from the FLUXNET2015 dataset (variable name: GPP_VUT_MEAN). We required all site-months to have over 75% valid GPP observations and required site-years to have a minimum of 9 months of data. We gridded the MCD43A4.006 dataset

to 0.5° by averaging all 500 meter pixels whose center fell within each 0.5° grid cell for the global upscaling. No additional gap filling, apart from those procedures inherent in the production of the underlying daily reflectance values (see Schaaf et al., 2002), was used in regridding. Missingness of $NIR_V$ data at both the site and global scale due to quality control issues (e.g., clouds) was minimal (Fig. S1).

In addition to the site-level comparisons, we evaluated $NIR_V$-based GPP estimates against two existing models of GPP: FLUXCOM, a machine learning approach for upscaling FLUXNET observations (Tramontana et al., 2016), and the Breathing Earth System Simulator (BESS), a physiologically based land surface model that has been extensively benchmarked against eddy covariance measurements of GPP (Jiang et al., 2016; Ryu et al., 2011). For FLUXCOM, we used the mean ensemble of annual GPP_HB fluxes from FLUXCOM CRUNCEPv6, available from http://www.fluxcom.org/CF-Download/. For BESS, we used GPP from BESS V1, downloaded from http://environment.snu.ac.kr/bess_flux/. Site-level RMSE values for FLUXCOM and BESS were derived from data provided by the authors (Jiang et al., 2016; Tramontana et al., 2016). We compared models using an Akaike Information Criterion (AIC) based approach that simultaneously evaluates model accuracy and penalizes model complexity (see Supplementary Text 1 for details). AIC values were calculated for $NIR_V$, BESS, and FLUXCOM using only site-years shared across all three products.

## 2.2 Calibration

We used Bayesian estimation to relate $NIR_V$ and ecosystem type to GPP at both monthly and annual timescales. Bayesian estimation allowed us to fit slope and intercept, as well as hierarchical variance terms capturing site-level random effects (random deviations from the global slope and intercept per site) and error variance (Gelman et al., 1995). Because Bayesian estimation yields a joint posterior distribution of parameter estimates, upscaling from the model posterior allows us to accurately propagate multiple sources of uncertainty, including joint uncertainty in the model fixed structure (i.e. slope and intercept of the GPP $NIR_V$ relationship) and the random effects (i.e. unexplained site-to-site variation and residual variation in the training dataset). The best model, according to the Deviance Information Criteria (DIC; an AIC-like score modified for Bayesian models), consists of a single, near-zero y-intercept and differing slopes for evergreen, deciduous, and crop ecosystem types. The model includes two additional terms: a random site-level intercept term

and an error term, both of which were specified as normal distributions with mean of 0 and variance exponentially related to $NIR_V$. See Supplementary Text and Table S1 for a full description of the model structure and the Markov chain Monte Carlo fitting procedure, as well as alternative model structures tested. We performed ecosystem type-stratified ten-fold cross-validation at the site level (e.g., leaving out 20% of sites from each ecosystem type) to confirm that the final model was not overfit (Fig. S2). Calibration sites were distributed throughout the global range of observed annual $NIR_V$, though there were only three sites with annual $NIR_V$ above 2.5 (Fig. S3). In total, the final calibration dataset included data from 105 eddy covariance sites, comprising 526 site-years.

### 2.3 Upscaling

We produced global annual estimates of GPP using 1000 samples from the joint model posterior for all 0.5° vegetated land pixels from 2005 to 2015. For each posterior sample (i.e. each joint set of scaling and variance parameter estimates), we calculated per-pixel GPP using the scaling parameters for the ecosystem type, a random draw from the site-level error distribution for each pixel and a random draw from the residual error distribution for each pixel-year. Using the site-level model for our global upscaling captured correlations between parameter estimates (scaling slope and site-level variance estimates were often correlated), resulting in GPP estimates that appropriately represent statistical, site, and residual uncertainty from the full joint posterior distribution of the model. We present the median and 95% credible intervals from the distribution of the 1000 global GPP estimates.

## 3 Results & Discussion

### 3.1 Site-level Validation

$NIR_V$, combined with information on ecosystem type (deciduous, evergreen, and crop) explained 68% of the variation in annual GPP at 105 eddy covariance monitoring sites (526 site-years that passed quality-control and data completeness requirements) and had an RMSE of 0.36 kg C $m^{-2}$ $y^{-1}$ (Fig. 1). At the monthly scale, the same model explained 56% of monthly variation in GPP with an RMSE of 0.08 kg C $m^{-2}$ $mo^{-1}$ (Fig. 1, inset). At the annual scale, we found that the normalized difference vegetation index (NDVI) and the fraction of absorbed photosynthetic radiation (fPAR) (two popular vegetation indices) were worse predictors than $NIR_V$, explaining 59% and 52% percent

of the variation in annual GPP fluxes. The accuracy of $NIR_V$ far exceeded both NDVI and fPAR in terms of RMSE (Table S2). Importantly, the $NIR_V$-GPP relationship was consistently linear across all values of GPP (Fig. S4). The most parsimonious model included just three ecosystem types, with a single intercept and separate $NIR_V$-GPP slopes for sites with i) evergreen, ii) deciduous, and iii) crop ecosystem types. The model also accounted for variance in both residual error and site-level random intercepts that increased as a function of $NIR_V$ (Fig. S5). Dividing ecosystems into a greater number of types resulted in minor model improvements, but an almost identical DIC with more parameters, causing us to adopt the simpler three ecosystem type model.

The site-level performance of $NIR_V$-derived GPP compared favorably against BESS and FLUXCOM, when evaluated across overlapping site-years (Fig. 1B). The RMSE of site-level NIRv-based GPP estimates was 42% lower than estimates from BESS and 57% higher than estimates from FLUXCOM, the machine learning-based upscaling product. However, taking model complexity into account by using the Akaike Information Criterion (AIC) and using conservatively low estimates for number of fitted parameters in the alternative approaches, the $NIR_V$ approach had a far lower AIC than either BESS or FLUXCOM. This indicates that $NIR_V$ better balances model accuracy against model complexity and thereby has a lower likelihood of overfitting the site-level data. Strong performance at validation sites, especially relative to leading statistical and physiological based estimates of GPP, demonstrates that $NIR_V$ provides a robust basis for global estimates of GPP.

Furthermore, the $NIR_V$ approach requires no additional information on meteorological conditions, such as site temperature, vapor pressure deficit, or incoming radiation. Residuals in observed GPP relative to $NIR_V$-derived GPP estimates showed only weak relationships with meteorological variables (Fig. 2). For site-years with especially high values of annual precipitation, model accuracy was slightly improved by including precipitation in the model. Similarly, compound meteorological indices, like the ratio of precipitation to potential evapotranspiration ("aridity index") had only a weak relationship with GPP residuals (Fig. S7). Including all available meteorological data boosted $R^2$ by only 0.04, from 0.68 to 0.72 (Table S3), but led to a higher DIC, which indicates that the base $NIR_V$ model better generalizes for predictive purposes. Models combining individual meteorological variables with $NIR_V$ showed similar small improvements in $R^2$ and RMSE, accompanied by increased DIC.

Interestingly, model residuals had only a weak relationship with annual PAR (Fig. 2D, p=0.01, $R^2$=0.01). Light is the primary driver of photosynthesis at shorter time scales, suggesting that it should be the leading candidate for improving model predictions. This was not the case for estimates

A

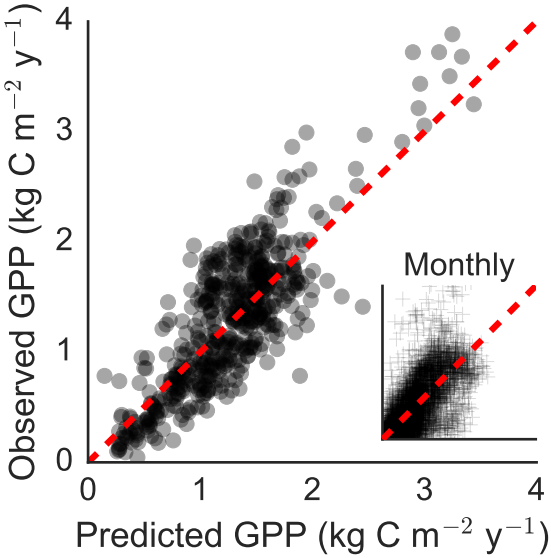


B

| GPP Product | RMSE (kg C m$^{-2}$ y$^{-1}$) | AIC |
|---|---|---|
| $NIR_V$ | 0.36 | 1736 |
| BESS | 0.55 | [1837, 1937] |
| FLUXCOM | 0.20 | 2013 |

**Figure 1.** $NIR_V$ explains a substantial portion of site-level GPP at both the monthly and annual timescale. Note the relatively large variation in monthly GPP estimates for low values of observed GPP, as compared to the near-zero intercept in the case of annual fluxes.

based on integrated $NIR_V$. In fact, including data on integrated PAR decreased the strength of the $NIR_V$-GPP relationship (Figs. S4D and S6). Such a pattern could result from $NIR_V$ already integrating relevant information about site-level radiation or have more to do with the uncertainties inherent in global radiation observations. We also found that model residuals at the annual time scale had no relationship with site-level cloudiness, indicating that $NIR_V$ alone captured the integrated effect of seasonal variation in sunny and cloudy conditions without the need for separately considering PAR (Fig. S8). By requiring fewer inputs, $NIR_V$-based upscaling of GPP reduces uncertainty from those inputs. It also allows the approach to be applied across a wide range of spatial and temporal scales where such data might not be available.

## 3.2 Global Upscaling

Applying the site-level scaling to globally resolved measurements of $NIR_V$, we estimated the median value of global annual GPP from 2003 to 2015 to be 147 Pg C y$^{-1}$, with a 95% credible interval of

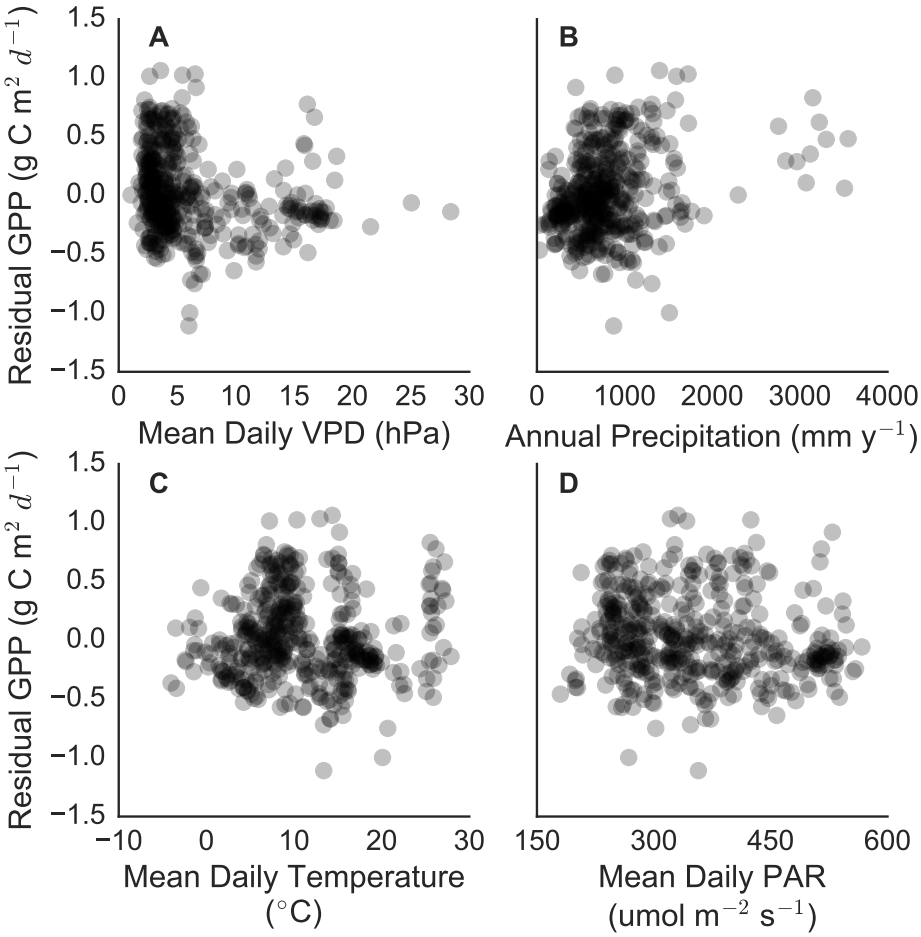


**Figure 2.** Model residuals of predicted GPP show no strong, systematic variations with site-level meteorological variables. As a result, using meteorological data in conjunction with $NIR_V$ reduces model generality (Table S3). This indicates that $NIR_V$ already captures the dominant influences of climate on canopy development.

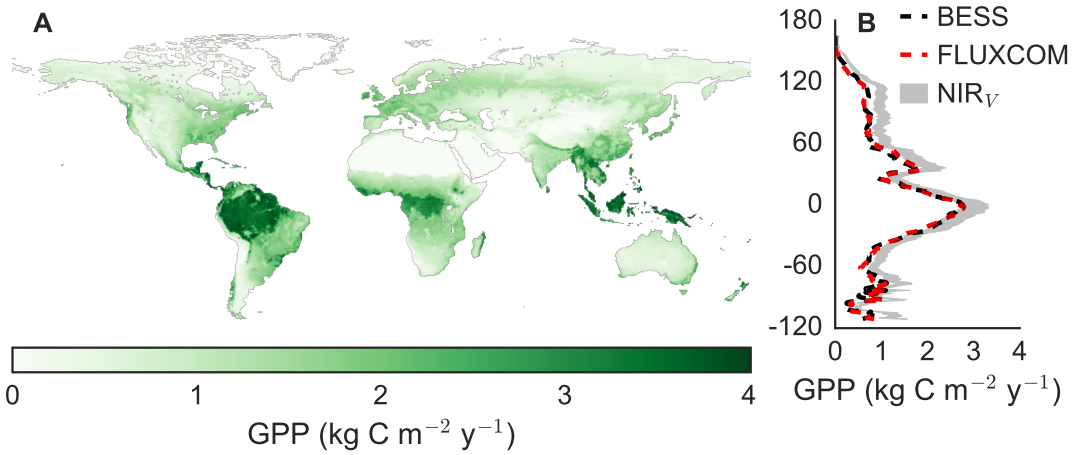


**Figure 3.** The A) global and B) latitudinal distribution of $NIR_V$-derived GPP. Estimates represent the median of 1000 nearly independent upscalings of $NIR_V$, while the full 95% credible range of GPP is shaded in grey for latitudinal estimates (latitude shown on the y-axis). The latitudinal distribution of annual GPP from FLUXCOM and BESS are shown for comparison.

131-163 Pg C y$^{-1}$. This median GPP estimate is intermediate between estimates from bottom-up models and constraints from $O_2$ isotopes. FLUXCOM places annual GPP at 118 Pg C y$^{-1}$, while BESS puts mean global GPP at 122 Pg C y$^{-1}$. Based on a meta-analysis, the full range of terrestrial ecosystem models estimate annual to be between 119 and 169 Pg C y$^{-1}$ (Anav et al., 2015). The Multi-Scale Synthesis and Terrestrial Model Intercomparison Project (MsTMIP) provides a similar range of estimates across 15 different terrestrial ecosystem models, with our $NIR_V$-derived GPP estimate falling on the high side of those model estimates (Fig. S9). $O_2$ isotopic measurements are consistent with global annual GPP in the range of 150 to 175 Pg C y$^{-1}$ (Welp et al., 2011).

The spatial distribution of $NIR_V$-derived GPP is broadly consistent with previous global GPP estimates (Fig. 3). As expected, GPP is concentrated in the tropics and declines toward the poles. On a per biome basis, tropical forests contribute the most, accounting for 31% of global GPP; FLUXCOM and BESS attribute 34% and 33% of GPP to tropical forests, respectively. Though lower in relative terms, $NIR_V$-derived GPP in tropical forests is 15% higher than both FLUXCOM and BESS GPP estimates. Differences were even larger at higher latitudes, where $NIR_V$ assigns higher productivity to midlatitude mixed forests, grasslands, and shrub-dominated ecosystems (Fig. 3B; Table S4). One explanation for this pattern is that $NIR_V$ minimizes soil contamination that might cause alternative remote sensing approaches to systematically underestimate leaf area across the midlatitudes. Consistent with this view, a recent study that combined solar-induced chlorophyll fluorescence with a terrestrial ecosystem model reports similar relative increases in extratropical

GPP (Norton et al., 2018).

On a per pixel basis, $NIR_V$ GPP estimates are strongly linear with GPP estimates from both FLUXCOM and BESS at the annual time scale. $R^2$ exceeds 0.90 and RMSE is below 0.4 kg C $m^{-2}$ $y^{-1}$ for both products (Fig. S11). Comparison of $NIR_V$ to GPP estimates from the MODIS GPP algrorithm shows similar performance (Fig. S12). This consistency is striking, given that the $NIR_V$ approach requires only two inputs ($NIR_V$ and ecosystem type). By contrast, both FLUXCOM and BESS require numerous environmental inputs. While broadly consistent, the comparison also emphasizes that $NIR_V$-derived GPP estimates are typically higher, exceeding FLUXCOM GPP by a median value of 0.24 kg C $m^{-2}$ $y^{-1}$ and BESS GPP by 0.21 kg C $m^{-2}$ $y^{-1}$. There is no obvious reason that $NIR_V$ might be biased high. It might be tempting to think that physiological stress, which is not explicitly accounted for by $NIR_V$, might explain the higher GPP from this approach. However, the $NIR_V$-based approach uses the annual sum of both $NIR_V$ and measured GPP, meaning $NIR_V$-derived GPP estimates are calibrated to include all of the stress effects at FLUXNET sites, when integrated to the annual scale. Such an interpretation is supported by the weak correlations between model residual GPP and numerous meteorological variables. If $NIR_V$ failed to capture the effects of lower precipitation or higher VPD on plant productivity, we would expect these environmental variables to explain additional variations in annual GPP. Yet meteorological variables provide little additional predictive power, meaning the annual $NIR_V$-based GPP estimates could be biased upwards only if FLUXNET sites are systematically biased toward low-stress locations or the FLUXNET2015 GPP estimates are biased towards good years where stress did not limit photosynthesis. Of course, such biases would affect any upscaling approach calibrated to the FLUXNET2015 dataset.

Similarly, using the same satellite data at both the site and global scales minimizes the likelihood that systematic errors or biases in the retrieval of $NIR_V$ affect our estimates of GPP; any error or bias in $NIR_V$ should be accounted for by our site-level calibration. There is little evidence for systematic biases in our model fit (Figs. 1 and S10). However, even in two worst-case scenarios of systematic bias (overprediction at low productivity sites or underprediction at high productivity sites), neither maximum credible bias would affect our annual global estimate by more than 10%, which is considerably smaller than the 30 Pg C $y^{-1}$ credible interval around our mean estimate and the differences between our estimate and either BESS or FLUXCOM (Fig S10). Alternatively, both BESS and FLUXCOM might systematically underestimate true GPP, an interpretation consistent with the constraint from oxygen isotopes (Welp et al., 2011). Resolving this discrepancy represents

an important next step in the study photosynthesis at the global scale.

### 3.3 Uncertainty Analysis

Model parsimony, combined with Bayesian estimation, allows us to propagate three sources of uncertainty for each pixel based on the uncertainties quantified in model calibration: statistical (variation in per ecosystem type scaling in the model posterior distribution), site (deviation of each pixel's intercept from the global relationship for that ecosystem type), and residual (otherwise unexplained error). Median per pixel uncertainty is 0.20 kg C $m^{-2}$ $y^{-1}$. Total uncertainty, comprising all three sources of error, peaks in the tropics where total annual $NIR_V$ is highest. In the worst case, the 95% credible interval of GPP exceeds 0.75 kg C $m^{-2}$ $y^{-1}$ in the Amazon basin and Indonesia (Fig. 4A). Given that tropical forests constitute the highest proportion of GPP (exceeding 30%) and have relatively few flux measurements, high uncertainty throughout the tropics significantly contributes to the overall uncertainty of global GPP estimates, regardless of approach.

Bayesian upscaling allows the uncertainties in parameter estimation from the site-level calibration to be projected globally; two examples of pixel-level uncertainties are shown in Fig. 4B. GPP estimated for each pixel fully contains the uncertainties present in the FLUXNET2015 dataset, providing added confidence in the robustness of credible range of estimated GPP. Outside of pixels with especially low $NIR_V$, statistical uncertainty is always lowest in both relative and absolute terms, indicating minimal uncertainty in per ecosystem type scaling. On average, site uncertainty is always largest, meaning there is more uncertainty in the $NIR_V$-GPP relationship from site to site (primarily in the site-level intercept, Fig. S5) than inter-annual variation (encompassed by residual uncertainty) in the $NIR_V$-GPP relationship at a single site. Site-to-site variability is randomly distributed, showing no relationship with site climate (Fig. S13), thus highlighting retrieval errors (e.g., soil reflectance, clouds) in $NIR_V$ and inherent uncertainties in eddy covariance derived GPP estimates as the likely cause of site-level uncertainty.

$NIR_V$ provides a novel approach for estimating GPP that combines a very simple formulation with excellent performance at validation sites (Fig. 1). As such, the $NIR_V$ approach is largely independent of existing semi-empirical and process-based upscaling approaches. Furthermore, the $NIR_V$ approach achieves strong quantification of uncertainties while maintaining parsimony. This combination of simple calculation plus straightforward analysis and partitioning of uncertainty between model structure and inputs makes $NIR_V$ a useful tool for revisiting and revising

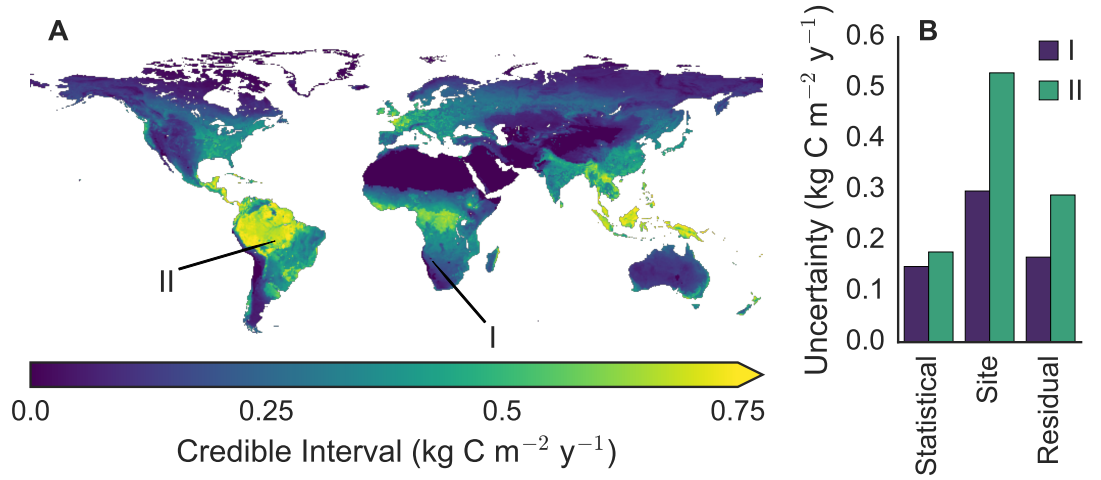


**Figure 4.** Bayesian hierarchical modeling allows for per pixel error estimation. A) Uncertainty in GPP peaks in the tropics (especially the Amazon and Indonesia), where the credible range of GPP exceed 0.75 kg C m$^{-2}$ y$^{-1}$. B) Uncertainty can be evaluated on a per pixel basis, where site-level uncertainty is typically largest.

long-standing assumptions about the global controls of photosynthesis.

The strong correlation of $NIR_V$ and GPP at FLUXNET calibration sites provides *prima facie* evidence for the hypothesis that plants allocate resources such that the potential to harvest light (controlled by canopy architecture) and the potential for $CO_2$ fixation (controlled by physiology and biochemical capacity) are held in balance. To further test this hypothesis, we examined differences in the strength of the $NIR_V$-GPP relationship at successively longer integration times for evergreen and deciduous validation sites. Relative to evergreens, deciduous leaves have higher photosynthetic rates and must recoup the cost of constructing leaves over a short period of time. Alternatively, evergreen canopies amortize the cost of leaf construction and maintenance over a year or more and, as a result, have less flexibility to respond to short-term perturbations in resource availability (Chabot et al., 1982). Given these contrasting strategies, we expect that $NIR_V$ at deciduous sites should track GPP just as well at short time scales as it does at longer time scales, while as integration time increases from days to months, the performance of $NIR_V$ as a predictor of GPP should increase at evergreen sites. This is exactly the pattern found at the FLUXNET validation sites, which we tested using Bonferroni adjusted t-tests (Fig. 5). At deciduous sites, $NIR_V$ is no more powerful at explaining daily GPP fluxes than it is at explaining fluxes integrated to 90 days ($p > 0.05$, Bonferroni adjusted). While at evergreen sites, $NIR_V$ is a significantly stronger predictor of GPP at 90 days than at the daily time scale ($p < 0.001$; Bonferroni adjusted). Interestingly, by seven days, the difference in performance between deciduous and evergreen sites is statistically indistinguishable ($p > 0.05$;

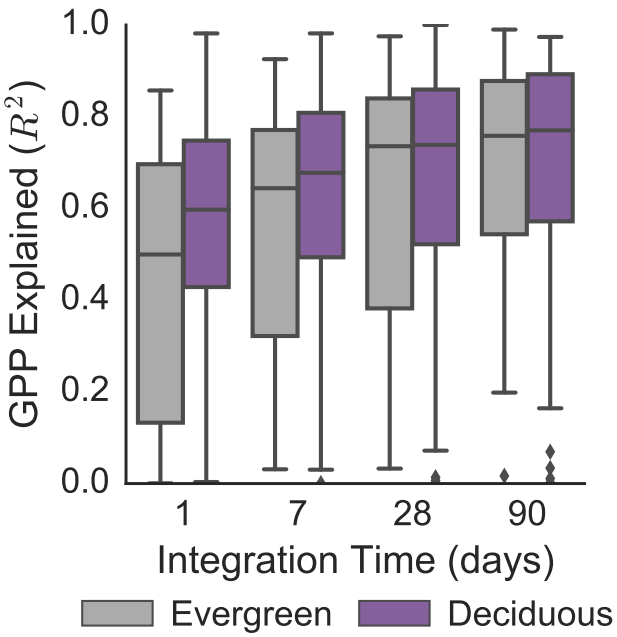


**Figure 5.** The $NIR_V$-GPP relationship for deciduous and evergreen canopies at numerous time scales. Deciduous canopies, which require more rapid payback on investments into light capture, exhibit the predicted pattern of more tightly tracking GPP at shorter time scales. Evergreen canopies, which amortize the cost of light capture over multiple years, can afford longer integration times when matching light capture to the availability of other resources.

Bonferroni adjusted).

The coupling of $NIR_V$ and GPP even holds during drought events. During the 2012 North American drought, $NIR_V$ showed characteristic early spring green-up, conforming with the spring-ward shift of both carbon and water fluxes documented by Wolf et al. (2016). With the onset of drought at severely drought affected site US-MMS, both $NIR_V$ and GPP rapidly declined in parallel, resulting in a similar $NIR_V$-GPP relationship as that of non-drought years (Figs. S14A and S14B). Thus, the coupling between the components of canopy structure that influence NIR reflectance and stress-constrained canopy photosynthetic capacity remains strong even at the short timescale of acute stress events. Notably, NDVI showed little deviation compared to non-drought years during the same period (Fig. S14C). The extent of the coupling between canopy structure and productivity at sub-annual time scales likely varies by ecosystem type, making the study of $NIR_V$-GPP dynamics under drought conditions an important area of future study.

On an instantaneous basis, environmental factors like water, light, and temperature combine with leaf-level biochemical capacity to dictate the rate of photosynthesis (Farquhar et al., 1980). The accuracy of $NIR_V$ for estimating GPP, without the need for additional inputs like total incoming

radiation (Fig. 2), does not imply that environmental factors are irrelevant to photosynthesis, but rather that, when integrated over the appropriate time interval, canopy architecture and the physiological controls on photosynthesis are coordinated. This interpretation of the $NIR_V$-GPP relationship also helps explain why including meteorological data does little to improve the accuracy of $NIR_V$-derived GPP estimates. If integrated levels of temperature, light, and water availability (as well as nutrients) jointly determine canopy development and physiological potential, then canopy structure, as summarized by $NIR_V$, should contain the information necessary to accurately estimate GPP. The minor improvement from including meteorological data likely indicates that no single linear relationship between one or even multiple meteorological variables accounts for the large number of possible combinations of meteorology and plant response (Fig. 2 and Table S3).

A major strength of the $NIR_V$ approach is that it allows statistically valid error propagation (Fig. 4). More complicated approaches for upscaling GPP make it difficult to accurately partition sources of error, especially model structural errors and errors due to input uncertainties. FLUXCOM, for example, functionally operates as a black box, limiting our ability to draw biological inferences about the global controls of GPP from the model itself. With the $NIR_V$-based approach, three sources of error warrant consideration. First, it could be the case that even though $NIR_V$ captures many of the controls of GPP, the slowly shifting integrator of $NIR_V$ might contain delays and inconsistencies that introduce uncertainties in the $NIR_V$-GPP relationship. Second, the coordination of structure and physiology might be imprecise, failing to account for some of the factors that influence GPP. Third, there are almost certainly measurement errors in the $NIR_V$ and GPP datasets used for calibration. The latter two possibilities are strongly suggested by the predominance of site-level error (Fig. 4B and Fig. S5), which indicates that either the physiology controlling the $NIR_V$-GPP relationship varies from site to site or that the $NIR_V$ measurements and/or GPP measurements used for calibration lack consistency across space. As a result, efforts to improve both the robustness of measurements of $NIR_V$ (e.g., better cloud filtering) and eddy covariance derived estimates of GPP (e.g., how GPP is partitioned from net ecosystem exchange, the mismatch between flux footprints and satellite measurements) are essential to minimizing site-level error.

A clear illustration of problems with the MODIS data used to calculate $NIR_V$ comes from GF-Guy, an eddy covariance site in French Guyana. GPP fluxes at GF-Guy varied less than 20% month to month, while $NIR_V$ varied by a factor of three (Fig. 6A), which suggests errors in MODIS observations at the site. A likely explanation is cloud contamination, as remote sensing in the tropics is notoriously plagued by clouds. To investigate this, we used the multi-angle implementation of

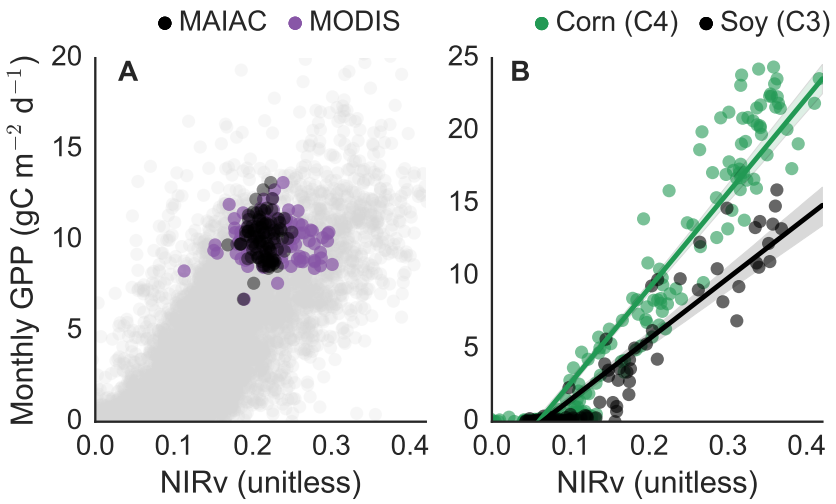


**Figure 6.** Parsimony allows for the investigation of sources of model uncertainty. A) Cloud contamination drives large monthly variations in MODIS collection 6 $NIR_V$ that are not matched by variations in $NIR_V$. All monthly data from the FLUXNET2015 dataset shown in grey. B) Photosynthetic pathway predictably alters the $NIR_V$-GPP relationship, as C4 plants have greater efficiency.

atmospheric correction for MODIS (MAIAC) data product, newly available for selected sites. MAIAC uses atmospheric modeling to remove aerosols, sub-pixel clouds, and other artifacts from MODIS satellite imagery (Lyapustin et al., 2011). The variability of $NIR_V$ dramatically decreased with the MAIAC data (Fig. 6A). In fact, MAIAC-derived $NIR_V$ had a smaller dynamic range than measured GPP, strongly indicating cloud contamination of the baseline MODIS dataset at GF-Guy and, in all likelihood, throughout the tropics. Unfortunately, the 250 meter resolution MAIAC data needed to perform site-level calibration are not yet available for all FLUXNET sites. Cloud contamination in the MODIS data likely causes systematic underestimation of $NIR_V$ throughout the tropics, which in turn would bias our median global GPP estimate upward and make 147 Pg C $y^{-1}$ a conservative estimate of global GPP.

Fundamental differences in plant physiology can also contribute to site uncertainty. One clear candidate is the difference in C3 and C4 photosynthesis. C4 plants fix $CO_2$ more efficiently than C3 plants, which should cause a steeper slope in the $NIR_V$-GPP relationship, all else equal. Tests at a trio of Nebraskan eddy covariance towers that annually rotate between soy (C3) and corn (C4) crops, reveal significant differences in the $NIR_V$-GPP slope with crop type (Fig. 6B). Including information on the distribution of C3 and C4 vegetation across both wild and managed ecosystems should decrease uncertainty. It would also likely increase the median estimate of GPP, as C3 sites comprise the majority of the calibration dataset, further emphasizing the conservative nature of the 147 Pg C

$y^{-1}$ estimate of GPP.

A third advantage of the $NIR_V$ approach is that it can be calculated from existing high-resolution and widely available satellite imagery. This makes $NIR_V$ immediately available for detailed studies and trend analyses at a wide variety of spatial and temporal scales, from individual study sites to the entire globe (Figs. 1 and 3). Our approach for estimating GPP from $NIR_V$ could also be calculated for the full Landsat and MODIS records, as well as the 39-year record of the Advanced Very High Resolution Radiometer (AVHRR) series of sensors (Tucker et al., 2005). Finally, the ease of measuring $NIR_V$ allows researchers to make inexpensive, canopy-scale spectral measurements that are directly comparable with satellite data, facilitating efforts to bridge spatial scales.

To conclude, $NIR_V$ provides a new, largely independent approach for estimating global GPP with excellent performance at FLUXNET calibration sites. The median estimate from this approach, 147 Pg C $y^{-1}$, is higher than recent estimate from bottom-up process-based models but is lower than global constraints from oxygen isotopes. Correcting known sources of uncertainty will likely increase the median estimate. In addition to high accuracy at calibration sites, the approach combines simple calculation, robust error propagation, and the ability to utilize decades of historical remote sensing data. Future refinements of the $NIR_V$-based approach can come from improved remote sensing inputs and inclusion of additional physiological processes.

# References


Ammann, Ch, CR Flechard, J Leifeld, A Neftel, and J Fuhrer (2007). "The carbon budget of newly established temperate grassland depends on management intensity". *Agriculture, Ecosystems & Environment* 121.1-2, pp. 5–20.

Anav, Alessandro, Pierre Friedlingstein, Christian Beer, Philippe Ciais, Anna Harper, Chris Jones, Guillermo Murray-Tortarolo, Dario Papale, Nicholas C Parazoo, Philippe Peylin, et al. (2015). "Spatiotemporal patterns of terrestrial gross primary production: A review". *Reviews of Geophysics* 53.3, pp. 785–818.

Aubinet, Marc, B Chermanne, M Vandenhaute, Bernard Longdoz, M Yernaux, and E Laitat (2001). "Long term carbon dioxide exchange above a mixed forest in the Belgian Ardennes". *Agricultural and Forest Meteorology* 108.4, pp. 293–315.

Badgley, Grayson, Christopher B Field, and Joseph A Berry (2017). "Canopy near-infrared reflectance and terrestrial photosynthesis". *Science Advances* 3.3, e1602244.

Baldocchi, Dennis (2008). "'Breathing' of the terrestrial biosphere: lessons learned from a global network of carbon dioxide flux measurement systems". *Australian Journal of Botany* 56.1, pp. 1–26.

Baldocchi, Dennis D, Liukang Xu, and Nancy Kiang (2004). "How plant functional-type, weather, seasonal drought, and soil physical properties alter water and energy fluxes of an oak–grass savanna and an annual grassland". *Agricultural and Forest Meteorology* 123.1-2, pp. 13–39.

Baldocchi, Dennis, Eva Falge, Lianhong Gu, Richard Olson, David Hollinger, Steve Running, Peter Anthoni, Ch Bernhofer, Kenneth Davis, Robert Evans, et al. (2001). "FLUXNET: A new tool to study the temporal and spatial variability of ecosystem-scale carbon dioxide, water vapor, and energy flux densities". *Bulletin of the American Meteorological Society* 82.11, pp. 2415–2434.

Beer, Christian, Markus Reichstein, Enrico Tomelleri, Philippe Ciais, Martin Jung, Nuno Carvalhais, Christian Rödenbeck, M Altaf Arain, Dennis Baldocchi, Gordon B Bonan, et al. (2010). "Terrestrial gross carbon dioxide uptake: global distribution and covariation with climate". *Science*, p. 1184984.

Bergeron, Onil, Hank A Margolis, T Andrew Black, Carole Coursolle, Allison L Dunn, Alan G Barr, and Steven C Wofsy (2007). "Comparison of carbon dioxide fluxes over three boreal black spruce forests in Canada". *Global Change Biology* 13.1, pp. 89–107.

Beringer, Jason, Lindsay B Hutley, Jorg M Hacker, Bruno Neininger, et al. (2011). "Patterns and processes of carbon, water and energy cycles across northern Australian landscapes: From point to region". *Agricultural and Forest Meteorology* 151.11, pp. 1409–1416.

Billesbach, Dave and James Bradford (2016). *AmeriFlux US-AR1 ARM USDA UNL OSU Woodward Switchgrass 1*. Tech. rep. AmeriFlux; US Department of Agriculture; University of Nebraska.

Bloom, Arnold J, F Stuart Chapin, and Harold A Mooney (1985). "Resource limitation in plants - an economic analogy". *Annual Review of Ecology and Systematics* 16, pp. 363–392.

Bonal, Damien, Alexandre Bosc, Stéphane Ponton, JEAN-YVES GORET, Benoıt Burban, Patrick Gross, JEAN-MARC BONNEFOND, JAN Elbers, Bernard Longdoz, Daniel Epron, et al. (2008). "Impact of severe dry season on net ecosystem exchange in the Neotropical rainforest of French Guiana". *Global Change Biology* 14.8, pp. 1917–1933.

Bonan, Gordon B, Peter J Lawrence, Keith W Oleson, Samuel Levis, Martin Jung, Markus Reichstein, David M Lawrence, and Sean C Swenson (2011). "Improving canopy processes in the Community Land Model version 4 (CLM4) using global flux fields empirically inferred from FLUXNET data". *Journal of Geophysical Research: Biogeosciences* 116.G2.

Carrara, Arnaud, Andrew S Kowalski, Johan Neirynck, Ivan A Janssens, Jorge Curiel Yuste, and Reinhart Ceulemans (2003). "Net ecosystem CO2 exchange of mixed forest in Belgium over 5 years". *Agricultural and Forest Meteorology* 119.3-4, pp. 209–227.

Cescatti, ALESSANDRO and ROBERTO ZORER (2003). "Structural acclimation and radiation regime of silver fir (Abies alba Mill.) shoots along a light gradient". *Plant, Cell & Environment* 26.3, pp. 429–442.

Ceschia, Eric, Pierre Béziat, Jean-François Dejoux, Marc Aubinet, Ch Bernhofer, Bernard Bodson, Nina Buchmann, Arnaud Carrara, Pierre Cellier, Paul Di Tommasi, et al. (2010). "Management effects on net ecosystem carbon and GHG budgets at European crop sites". *Agriculture, Ecosystems & Environment* 139.3, pp. 363–383.

Chabot, Brian F and David J Hicks (1982). "The ecology of leaf life spans". *Annual review of ecology and systematics* 13.1, pp. 229–259.

Chen, Shiping, Jiquan Chen, Guanghui Lin, Wenli Zhang, Haixia Miao, Long Wei, Jianhui Huang, and Xingguo Han (2009). "Energy balance and partition in Inner Mongolia steppe ecosystems with different land use types". *Agricultural and Forest Meteorology* 149.11, pp. 1800–1809.

Cook, Bruce D, Kenneth J Davis, Weiguo Wang, Ankur Desai, Bradford W Berger, Ron M Teclaw, Jonathan G Martin, Paul V Bolstad, Peter S Bakwin, Chuixiang Yi, et al. (2004). "Carbon exchange and venting anomalies in an upland deciduous forest in northern Wisconsin, USA". *Agricultural and Forest Meteorology* 126.3-4, pp. 271–295.

Delpierre, Nicolas, Daniel Berveiller, Elena Granda, and Eric Dufrene (2016). "Wood phenology, not carbon input, controls the interannual variability of wood growth in a temperate oak forest." *The New phytologist* 210 2, pp. 459–70.

Desai, Ankur R, Paul V Bolstad, Bruce D Cook, Kenneth J Davis, and Eileen V Carey (2005). "Comparing net ecosystem exchange of carbon dioxide between an old-growth and mature forest in the upper Midwest, USA". *Agricultural and Forest Meteorology* 128.1-2, pp. 33–55.

Desai, Ankur R., Ke Xu, Hanqin Tian, Peter Weishampel, Jonathan Thom, Dan Baumann, Arlyn E. Andrews, Bruce D. Cook, Jennifer Y. King, and Randall Kolka (2015). "Landscape-level terrestrial methane flux observed from a very tall tower". *Agricultural and Forest Meteorology* 201, pp. 61–75. ISSN: 0168-1923.

Dolman, AJ, EJ Moors, and JA Elbers (2002). "The carbon uptake of a mid latitude pine forest growing on sandy soil". *Agricultural and Forest Meteorology* 111.3, pp. 157–170.

Dong, Gang, Jixun Guo, Jiquan Chen, Ge Sun, Song Gao, Liangjun Hu, and Yunlong Wang (2011). "Effects of spring drought on carbon sequestration, evapotranspiration and water use efficiency in the Songnen meadow steppe in northeast China". *Ecohydrology* 4.2, pp. 211–224.

Eamus, Derek, James Cleverly, Nicolas Boulain, Nicole Grant, Ralph Faux, and Randol Villalobos-Vega (2013). "Carbon and water fluxes in an arid-zone Acacia savanna woodland: An analyses of seasonal patterns and responses to rainfall events". *Agricultural and Forest Meteorology* 182, pp. 225–238.

Eugster, Werner and Matthias J Zeeman (2006). "Micrometeorological techniques to measure ecosystem-scale greenhouse gas fluxes for model validation and improvement". *International Congress Series*. Vol. 1293. Elsevier, pp. 66–75.

Fares, Silvano and Francesco Loreto (2015). "Isoprenoid emissions by the Mediterranean vegetation in Castelporziano". *Rendiconti Lincei* 26.3, pp. 493–498.

Farquhar, Graham D, Susan von Caemmerer, and Joseph A Berry (1980). "A biochemical model of photosynthetic CO2 assimilation in leaves of C3 species". *Planta* 149.1, pp. 78–90.

Ferréa, Chiara, Terenzio Zenone, Roberto Comolli, and Günther Seufert (2012). "Estimating heterotrophic and autotrophic soil respiration in a semi-natural forest of Lombardy, Italy". *Pedobiologia* 55.6, pp. 285–294.

Field, Christopher B, James T Randerson, and Carolyn M Malmström (1995). "Global net primary production: combining ecology and remote sensing". *Remote sensing of Environment* 51.1, pp. 74–88.

Fischer, Marc L, David P Billesbach, Joseph A Berry, William J Riley, and Margaret S Torn (2007). "Spatiotemporal variations in growing season exchanges of CO2, H2O, and sensible heat in agricultural fields of the Southern Great Plains". *Earth Interactions* 11.17, pp. 1–21.

Fu, Yu-Ling, Gui-Rui Yu, Xiao-Min Sun, Ying-Nian Li, Xue-Fa Wen, Lei-Ming Zhang, Zheng-Quan Li, Liang Zhao, and Yan-Bin Hao (2006). "Depression of net ecosystem CO2 exchange in semi-arid Leymus chinensis steppe and alpine shrub". *Agricultural and Forest Meteorology* 137.3-4, pp. 234–244.

Galvagno, M, G Wohlfahrt, E Cremonese, M Rossini, R Colombo, G Filippa, T Julitta, G Manca, C Siniscalco, U Morra di Cella, et al. (2013). "Phenology and carbon dioxide source/sink strength of a subalpine grassland in response to an exceptionally short snow season". *Environmental Research Letters* 8.2, p. 025008.

Gelman, Andrew, John B Carlin, Hal S Stern, and Donald B Rubin (1995). *Bayesian data analysis*. Chapman and Hall/CRC.

Gilmanov, TG, JF Soussana, L Aires, V Allard, C Ammann, M Balzarolo, Z Barcza, C Bernhofer, CL Campbell, A Cernusca, et al. (2007). "Partitioning European grassland net ecosystem CO2 exchange into gross primary productivity and ecosystem respiration using light response function analysis". *Agriculture, ecosystems & environment* 121.1-2, pp. 93–120.

Goldstein, AH, NE Hultman, JM Fracheboud, MR Bauer, JA Panek, M Xu, Y Qi, AB Guenther, and W Baugh (2000). "Effects of climate variability on the carbon dioxide, water, and sensible heat fluxes above a ponderosa pine plantation in the Sierra Nevada (CA)". *Agricultural and Forest Meteorology* 101.2-3, pp. 113–129.

Gough, Christopher M., Brady S. Hardiman, Lucas E. Nave, Bohrer Gil, Maurer Kyle D., Vogel Christoph S., Nadelhoffer Knute J., and Curtis Peter S. (2013). "Sustained carbon uptake and storage following moderate disturbance in a Great Lakes forest". *Ecological Applications* 23.5, pp. 1202–1215.

Goulden, Michael L, Gregory C Winston, ANDREW MS McMILLAN, Marcy E Litvak, Edward L Read, Adrian V Rocha, and J Rob Elliot (2006). "An eddy covariance mesonet to measure the effect of forest age on land–atmosphere exchange". *Global Change Biology* 12.11, pp. 2146–2162.

Goward, Samuel N, Compton J Tucker, and Dennis G Dye (1985). "North American vegetation patterns observed with the NOAA-7 advanced very high resolution radiometer". *Vegetatio* 64.1, pp. 3–14.

GrüNwald, Thomas and Christian Bernhofer (2007). "A decade of carbon, water and energy flux measurements of an old spruce forest at the Anchor Station Tharandt". *Tellus B: Chemical and Physical Meteorology* 59.3, pp. 387–396.

Hatala, Jaclyn A., Matteo Detto, Oliver Sonnentag, Steven J. Deverel, Joseph Verfaillie, and Dennis D. Baldocchi (2012). "Greenhouse gas (CO2, CH4, H2O) fluxes from drained and flooded agricultural peatlands in the Sacramento-San Joaquin Delta". *Agriculture, Ecosystems Environment* 150, pp. 1–18. ISSN: 0167-8809.

Hommeltenberg, J., H. P. Schmid, M. Drösler, and P. Werle (2014). "Can a bog drained for forestry be a stronger carbon sink than a natural bog forest?" *Biogeosciences* 11.13, pp. 3477–3493.

Hoyer, S. and J. Hamman (2017). "xarray: N-D labeled arrays and datasets in Python". *Journal of Open Research Software* 5.1.

Hunter, John D (2007). "Matplotlib: A 2D graphics environment". *Computing in science & engineering* 9.3, pp. 90–95.

Jiang, Chongya and Youngryel Ryu (2016). "Multi-scale evaluation of global gross primary productivity and evapotranspiration products derived from Breathing Earth System Simulator (BESS)". *Remote Sensing of Environment* 186, pp. 528–547.

Jung, Martin, Markus Reichstein, Christopher R Schwalm, Chris Huntingford, Stephen Sitch, Anders Ahlström, Almut Arneth, Gustau Camps-Valls, Philippe Ciais, Pierre Friedlingstein, et al. (2017). "Compensatory water effects link yearly global land CO 2 sink changes to temperature". *Nature* 541.7638, pp. 516–520.

Karan, Mirko, Michael Liddell, Suzanne M Prober, Stefan Arndt, Jason Beringer, Matthias Boer, James Cleverly, Derek Eamus, Peter Grace, Eva Van Gorsel, et al. (2016). "The Australian SuperSite Network: A continental, long-term terrestrial ecosystem observatory". *Science of the Total Environment* 568, pp. 1263–1274.

Kato, Tomomichi, Yanhong Tang, Song Gu, Mitsuru Hirota, Mingyuan Du, Yingnian Li, and Xinquan Zhao (2006). "Temperature and biomass influences on interannual changes in CO2 exchange in an alpine meadow on the Qinghai-Tibetan Plateau". *Global Change Biology* 12.7, pp. 1285–1298.

Kluyver, Thomas, Benjamin Ragan-Kelley, Fernando Pérez, Brian Granger, Matthias Bussonnier, Jonathan Frederic, Kyle Kelley, Jessica Hamrick, Jason Grout, Sylvain Corlay, Paul Ivanov, Damián Avila, Safia Abdalla, and Carol Willing (2016). "Jupyter Notebooks – a publishing format for reproducible computational workflows". *Positioning and Power in Academic Publishing: Players, Agents and Agendas*. Ed. by F. Loizides and B. Schmidt. IOS Press, pp. 87–90.

Knohl, Alexander, Ernst-Detlef Schulze, Olaf Kolle, and Nina Buchmann (2003). "Large carbon uptake by an unmanaged 250-year-old deciduous forest in Central Germany". *Agricultural and Forest Meteorology* 118.3-4, pp. 151–167.

Kumar, Jitendra, Forrest M. Hoffman, William W. Hargrove, and Nathan Collier (2016). "Understanding the representativeness of FLUXNET for upscaling carbon flux from eddy covariance measurements". *Earth System Science Data Discussions*.

Kurbatova, J, C Li, A Varlagin, X Xiao, and N Vygodskaya (2008). "Modeling carbon dynamics in two adjacent spruce forests with different soil conditions in Russia". *Biogeosciences* 5.4, pp. 969–980.

Law, Beverly E., Dave Turner, John Campbell, Michael Lefsky, Michael Guzy, Osbert Sun, Steve Van Tuyl, and Warren Cohen (2006). "CARBON FLUXES ACROSS REGIONS: OBSERVATIONAL CONSTRAINTS AT MULTIPLE SCALES". In: *SCALING AND UNCERTAINTY ANALYSIS IN ECOLOGY*. Ed. by JIANGUO WU, K. BRUCE JONES, HARBIN LI, and ORIE L. LOUCKS. Dordrecht: Springer Netherlands, pp. 167–190. ISBN: 978-1-4020-4663-6.

Leuning, Ray, Helen A Cleugh, Steven J Zegelin, and Dale Hughes (2005). "Carbon and water fluxes over a temperate Eucalyptus forest and a tropical wet/dry savanna in Australia: measurements and comparison with MODIS remote sensing estimates". *Agricultural and Forest Meteorology* 129.3-4, pp. 151–173.

Loubet, Benjamin, Patricia Laville, Simon Lehuger, Eric Larmanou, Christophe Fléchard, Nicolas Mascher, Sophie Genermont, Romain Roche, Rossana M Ferrara, Patrick Stella, et al. (2011). "Carbon, nitrogen and Greenhouse gases budgets over a four years crop rotation in northern France". *Plant and Soil* 343.1-2, p. 109.

Lyapustin, Alexei, John Martonchik, Yujie Wang, Istvan Laszlo, and Sergey Korkin (2011). "Multiangle implementation of atmospheric correction (MAIAC): 1. Radiative transfer basis and look-up tables". *Journal of Geophysical Research: Atmospheres* 116.D3.

Ma, Siyan, Dennis D Baldocchi, Liukang Xu, and Ted Hehn (2007). "Inter-annual variability in carbon dioxide exchange of an oak/grass savanna and open grassland in California". *Agricultural and Forest Meteorology* 147.3-4, pp. 157–171.

Marcolla, Barbara, Alessandro Cescatti, Leonardo Montagnani, Giovanni Manca, Günther Kerschbaumer, and Stefano Minerbi (2005). "Importance of advection in the atmospheric CO2 exchanges of an alpine forest". *Agricultural and Forest Meteorology* 130.3-4, pp. 193–206.

Matteucci, Marco, Carsten Gruening, Ignacio Goded Ballarin, Guenther Seufert, and Alessandro Cescatti (2015). "Components, drivers and temporal dynamics of ecosystem respiration in a Mediterranean pine forest". *Soil Biology and Biochemistry* 88, pp. 224–235.

Mauder, Matthias, Matthias Cuntz, Clemens Drüe, Alexander Graf, Corinna Rebmann, Hans Peter Schmid, Marius Schmidt, and Rainer Steinbrecher (2013). "A strategy for quality and uncertainty assessment of long-term eddy-covariance measurements". *Agricultural and Forest Meteorology* 169, pp. 122–135.

McKinney, Wes et al. (2010). "Data structures for statistical computing in python". *Proceedings of the 9th Python in Science Conference*. Vol. 445. Austin, TX, pp. 51–56.

Migliavacca, Mirco, Michele Meroni, Giovanni Manca, Giorgio Matteucci, Leonardo Montagnani, Giacomo Grassi, Terenzio Zenone, Maurizio Teobaldelli, Ignacio Goded, Roberto Colombo, et al. (2009). "Seasonal and interannual patterns of carbon and water fluxes of a poplar plantation under peculiar eco-climatic conditions". *Agricultural and Forest Meteorology* 149.9, pp. 1460–1476.

Miller, Scott D, Michael L Goulden, Mary C Menton, Humberto R da Rocha, Helber C de Freitas, Cleilim Albert Dias de Sousa, et al. (2004). "Biometric and micrometeorological measurements of tropical forest carbon balance". *Ecological Applications* 14.sp4, pp. 114–126.

Monson, R. K., Turnipseed A. A., Sparks J. P., Harley P. C., Scott-Denton L. E., Sparks K., and Huxman T. E. (2002). "Carbon sequestration in a high-elevation, subalpine forest". *Global Change Biology* 8.5, pp. 459–478.

Monteith, John Lennox (1977). "Climate and the efficiency of crop production in Britain". *Philosophical Transactions of the Royal Society London B* 281.980, pp. 277–294.

Moureaux, Christine, Alain Debacq, Bernard Bodson, Bernard Heinesch, and Marc Aubinet (2006). "Annual net ecosystem carbon exchange by a sugar beet crop". *Agricultural and Forest Meteorology* 139.1-2, pp. 25–39.

Myneni, Ranga B., Forrest G. Hall, Piers J. Sellers, and Alexander L. Marshak (1995). "The interpretation of spectral vegetation indexes". *IEEE Transactions on Geoscience and Remote Sensing* 33.2, pp. 481–486.

Norton, A. J., P. J. Rayner, E. N. Koffi, M. Scholze, J. D. Silver, and Y.-P. Wang (2018). "Estimating global gross primary productivity using chlorophyll fluorescence and a data assimilation system with the BETHY-SCOPE model". *Biogeosciences Discussions* 2018, pp. 1–40.

Pilegaard, K, P Hummelshøj, NO Jensen, and Z Chen (2001). "Two years of continuous CO2 eddy-flux measurements over a Danish beech forest". *Agricultural and Forest Meteorology* 107.1, pp. 29–41.

Plummer, Martyn (2003). *JAGS: A program for analysis of Bayesian graphical models using Gibbs sampling*.

— (2013). "rjags: Bayesian graphical models using MCMC". *R package version* 3.10.

Posse, Gabriela, Nuria Lewczuk, Klaus Richter, and Piedad Cristiano (2016). "Carbon and water vapor balance in a subtropical pine plantation". *iForest-Biogeosciences and Forestry* 9.5, p. 736.

Potter, Christopher S, James T Randerson, Christopher B Field, Pamela A Matson, Peter M Vitousek, Harold A Mooney, and Steven A Klooster (1993). "Terrestrial ecosystem production: a process model based on global satellite and surface data". *Global Biogeochemical Cycles* 7.4, pp. 811–841.

Prober, Suzanne M, Kevin R Thiele, Philip W Rundel, Colin J Yates, Sandra L Berry, Margaret Byrne, Les Christidis, Carl R Gosper, Pauline F Grierson, Kristina Lemson, et al. (2012). "Facilitating adaptation of biodiversity to climate change: a conceptual framework applied to the world's largest Mediterranean-climate woodland". *Climatic Change* 110.1-2, pp. 227–248.

Rambal, S, R Joffre, JM Ourcival, J Cavender-Bares, and A Rocheteau (2004). "The growth respiration component in eddy CO2 flux from a Quercus ilex mediterranean forest". *Global Change Biology* 10.9, pp. 1460–1469.

Reverter, Borja R, EP Sánchez-Cañete, V Resco, Penelope Serrano-Ortiz, C Oyonarte, and Andrew S Kowalski (2010). "Analyzing the major drivers of NEE in a Mediterranean alpine shrubland". *Biogeosciences* 7.9, pp. 2601–2611.

Rey, Ana, Emiliano Pegoraro, Vanessa Tedeschi, Ilaria De Parri, Paul G Jarvis, and Riccardo Valentini (2002). "Annual variation in soil respiration and its components in a coppice oak forest in Central Italy". *Global Change Biology* 8.9, pp. 851–866.

Rockström, Johan, Will Steffen, Kevin Noone, Åsa Persson, F Stuart Chapin III, Eric F Lambin, Timothy M Lenton, Marten Scheffer, Carl Folke, Hans Joachim Schellnhuber, et al. (2009). "A safe operating space for humanity". *Nature* 461.7263, pp. 472–475.

Rothstein, David E., Donald. R. Zak, Kurt S. Pregitzer, and Peter S. Curtis (2000). "Kinetics of nitrogen uptake by Populus tremuloides in relation to atmospheric CO2 and soil nitrogen availability". *Tree Physiology* 20.4, pp. 265–270. eprint: `/oup/backfile/content_public/journal/treephys/20/4/10.1093/treephys/20.4.265/2/20-4-265.pdf`.

Ruehr, Nadine K, Jonathan G Martin, and Beverly E Law (2012). "Effects of water availability on carbon and water exchange in a young ponderosa pine forest: Above-and belowground responses". *Agricultural and forest meteorology* 164, pp. 136–148.

Running, Steven W (2012). "A measurable planetary boundary for the biosphere". *Science* 337.6101, pp. 1458–1459.

Running, Steven W and Ramakrishna R Nemani (1988). "Relating seasonal patterns of the AVHRR vegetation index to simulated photosynthesis and transpiration of forests in different climates". *Remote Sensing of Environment* 24.2, pp. 347–367.

Running, Steven W, Ramakrishna R Nemani, Faith Ann Heinsch, Maosheng Zhao, Matt Reeves, and Hirofumi Hashimoto (2004). "A continuous satellite-derived measure of global terrestrial primary production". *BioScience* 54.6, pp. 547–560.

Ryu, Youngryel, Dennis D Baldocchi, Hideki Kobayashi, Catharine van Ingen, Jie Li, T Andy Black, Jason Beringer, Eva Van Gorsel, Alexander Knohl, Beverly E Law, et al. (2011). "Integration of MODIS land and atmosphere products with a coupled-process model to estimate gross primary productivity and evapotranspiration from 1 km to global scales". *Global Biogeochemical Cycles* 25.4.

Sabbatini, S, N Arriga, T Bertolini, Simona Castaldi, T Chiti, C Consalvo, S Njakou Djomo, B Gioli, G Matteucci, and D Papale (2016). "Greenhouse gas balance of cropland conversion to bioenergy poplar short-rotation coppice". *Biogeosciences* 13.1, pp. 95–113.

Scanlon, T.M. and J.D. Albertson (2004). "Canopy scale measurements of CO2 and water vapor exchange along a precipitation gradient in southern Africa". *Global Change Biology* 10.3, pp. 329–341.

Schaaf, C and Z Wang (2015). "MCD43A4 MODIS/Terra+ Aqua BRDF/Albedo Nadir BRDF Adjusted RefDaily L3 Global 500 m V006". *NASA EOSDIS Land Processes DAAC*.

Schaaf, Crystal B., Feng Gao, Alan H. Strahler, Wolfgang Lucht, Xiaowen Li, Trevor Tsang, Nicholas C. Strugnell, Xiaoyang Zhang, Yufang Jin, and Jan-Peter Muller (2002). "First operational BRDF, albedo nadir reflectance products from MODIS". *Remote sensing of Environment* 83.1-2, pp. 135–148.

Schaefer, Kevin, Christopher R Schwalm, Chris Williams, M Altaf Arain, Alan Barr, Jing M Chen, Kenneth J Davis, Dimitre Dimitrov, Timothy W Hilton, David Y Hollinger, et al. (2012). "A model-data comparison of gross primary productivity: Results from the North American Carbon Program site synthesis". *Journal of Geophysical Research: Biogeosciences* 117.G3, G03010.

Schmid, Hans Peter, C Susan B Grimmond, Ford Cropley, Brian Offerle, and Hong-Bing Su (2000). "Measurements of CO2 and energy fluxes over a mixed hardwood forest in the mid-western United States". *Agricultural and Forest Meteorology* 103.4, pp. 357–374.

Scholes, R.J., N. Gureja, M. Giannecchinni, D. Dovie, B. Wilson, N. Davidson, K. Piggott, C. McLoughlin, K. Van Der Velde, A. Freeman, S. Bradley, R. Smart, and S. Ndala (2001). "The Environment and Vegetation of the Flux Measurement Site Near Skukuza". *Koedoe*, pp. 73–83.

Schroder, I (2014). "Arcturus Emerald OzFlux tower site". *OzFlux: Australian and New Zealand Flux Research and Monitoring, hdl* 102.100, p. 14249.

Scott, Russell (2016). *AmeriFlux US-Wkg Walnut Gulch Kendall Grasslands*. Tech. rep. AmeriFlux; United States Department of Agriculture.

Scott, Russell L (2010). "Using watershed water balance to evaluate the accuracy of eddy covariance evaporation measurements for three semiarid ecosystems". *Agricultural and Forest Meteorology* 150.2, pp. 219–225.

Scott, Russell L., Joel A. Biederman, Erik P. Hamerlynck, and Greg A. Barron-Gafford (2015). "The carbon balance pivot point of southwestern U.S. semiarid ecosystems: Insights from the 21st century drought". *Journal of Geophysical Research: Biogeosciences* 120.12, pp. 2612–2624. eprint: `https://agupubs.onlinelibrary.wiley.com/doi/pdf/10.1002/2015JG003181`.

Sellers, PJ, DA Randall, GJ Collatz, JA Berry, CB Field, DA Dazlich, C Zhang, GD Collelo, and L Bounoua (1996). "A revised land surface parameterization (SiB2) for atmospheric GCMs. Part I: Model formulation". *Journal of climate* 9.4, pp. 676–705.

Shao, Pu, Xubin Zeng, Koichi Sakaguchi, Russell K Monson, and Xiaodong Zeng (2013). "Terrestrial carbon cycle: climate relations in eight CMIP5 earth system models". *Journal of Climate* 26.22, pp. 8744–8764.

Sjöström, Martin, Jonas Ardö, Lars Eklundh, BA El-Tahir, HAM El-Khidir, Margareta Hellström, Petter Pilesjö, and Jonathan Seaquist (2009). "Evaluation of satellite based indices for gross primary production estimates in a sparse savanna in the Sudan". *Biogeosciences* 6.1, pp. 129–138.

Spano, Donatella, Pierpaolo Duce, Richard L Snyder, Pierpaolo Zara, and Andrea Ventura (2005). "Assessment of fuel dryness index on Mediterranean vegetation". *Proceedings of the 6th Symposium on Fire and Forest Meteorology, Cammore, Canada*.

Sturtevant, Cove, Benjamin L Ruddell, Sara Helen Knox, Joseph Verfaillie, Jaclyn Hatala Matthes, Patricia Y Oikawa, and Dennis Baldocchi (2016). "Identifying scale-emergent, nonlinear, asynchronous processes of wetland methane exchange". *Journal of Geophysical Research: Biogeosciences* 121.1, pp. 188–204.

Su, Yu-Sung and M Yajima (2015). "R2jags: Using R to run 'JAGS'". *R package version 0.5-7*.

Sulman, BN, AR Desai, BD Cook, N Saliendra, and DS Mackay (2009). "Contrasting carbon dioxide fluxes between a drying shrub wetland in Northern Wisconsin, USA, and nearby forests". *Biogeosciences* 6.6, pp. 1115–1126.

Team, R Core (2014). *R: A language and environment for statistical computing. R Foundation for Statistical Computing, Vienna, Austria. 2013*.

Tedeschi, Vanessa, ANA Rey, Giovanni Manca, Riccardo Valentini, Paul G Jarvis, and Marco Borghetti (2006). "Soil respiration in a Mediterranean oak forest at different developmental stages after coppicing". *Global Change Biology* 12.1, pp. 110–121.

Tramontana, Gianluca, Martin Jung, Christopher R Schwalm, Kazuhito Ichii, Gustau Camps-Valls, Botond Ráduly, Markus Reichstein, M Altaf Arain, Alessandro Cescatti, Gerard Kiely, et al. (2016). "Predicting carbon dioxide and energy fluxes across global FLUXNET sites with regression algorithms". *Biogeosciences*.

Tucker, Compton J, Jorge E Pinzon, Molly E Brown, Daniel A Slayback, Edwin W Pak, Robert Mahoney, Eric F Vermote, and Nazmi El Saleous (2005). "An extended AVHRR 8-km NDVI dataset compatible with MODIS and SPOT vegetation NDVI data". *International Journal of Remote Sensing* 26.20, pp. 4485–4498.

Tucker, Compton J, C Li Vanpraet, MJ Sharman, and Geri Van Ittersum (1985). "Satellite remote sensing of total herbaceous biomass production in the Senegalese Sahel: 1980–1984". *Remote sensing of environment* 17.3, pp. 233–249.

Urbanski, Shawn, C Barford, S Wofsy, C Kucharik, E Pyle, J Budney, K McKain, D Fitzjarrald, M Czikowsky, and JW Munger (2007). "Factors controlling CO2 exchange on timescales from hourly to decadal at Harvard Forest". *Journal of Geophysical Research: Biogeosciences* 112.G2.

Van der Molen, MK, JHC Gash, and JA Elbers (2004). "Sonic anemometer (co) sine response and flux measurement: II. The effect of introducing an angle of attack dependent calibration". *Agricultural and Forest Meteorology* 122.1-2, pp. 95–109.

Verma, Shashi B, Achim Dobermann, Kenneth G Cassman, Daniel T Walters, Johannes M Knops, Timothy J Arkebauer, Andrew E Suyker, George G Burba, Brigid Amos, Haishun Yang, et al. (2005). "Annual carbon dioxide exchange in irrigated and rainfed maize-based agroecosystems". *Agricultural and Forest Meteorology* 131.1-2, pp. 77–96.

Vesala, T, T Suni, Ü Rannik, P Keronen, T Markkanen, S Sevanto, T Grönholm, S Smolander, M Kulmala, H Ilvesniemi, et al. (2005). "Effect of thinning on surface fluxes in a boreal forest". *Global Biogeochemical Cycles* 19.2.

Vitale, Luca, Paul Di Tommasi, Guido D'Urso, and Vincenzo Magliulo (2016). "The response of ecosystem carbon fluxes to LAI and environmental drivers in a maize crop grown in two contrasting seasons". *International Journal of Biometeorology* 60.3, pp. 411–420. ISSN: 1432-1254.

Walt, Stéfan van der, S Chris Colbert, and Gael Varoquaux (2011). "The NumPy array: a structure for efficient numerical computation". *Computing in Science & Engineering* 13.2, pp. 22–30.

Waskom, Michael, Olga Botvinnik, Paul Hobson, John B. Cole, Yaroslav Halchenko, Stephan Hoyer, Alistair Miles, Tom Augspurger, Tal Yarkoni, Tobias Megies, Luis Pedro Coelho, Daniel Wehner, cynddl, Erik Ziegler, diego0020, Yury V. Zaytsev, Travis Hoppe, Skipper Seabold, Phillip Cloud, Miikka Koskinen, Kyle Meyer, Adel Qalieh, and Dan Allan (2014). *seaborn: v0.5.0 (November 2014)*.

Welp, Lisa R, Ralph F Keeling, Harro AJ Meijer, Alane F Bollenbacher, Stephen C Piper, Kei Yoshimura, Roger J Francey, Colin E Allison, and Martin Wahlen (2011). "Interannual variability in the oxygen isotopes of atmospheric CO 2 driven by El Niño". *Nature* 477.7366, pp. 579–582.

Williams, M, AD Richardson, M Reichstein, PC Stoy, P Peylin, Hans Verbeeck, N Carvalhais, M Jung, DY Hollinger, J Kattge, et al. (2009). "Improving land surface models with FLUXNET data". *Biogeosciences* 6.7, pp. 1341–1359.

Wilson, Adam M. and Walter Jetz (2016). "Remotely Sensed High-Resolution Global Cloud Dynamics for Predicting Ecosystem and Biodiversity Distributions". *PLOS Biology* 14.3, e1002415. ISSN: 1545-7885.

Wohlfahrt, Georg, Albin Hammerle, Alois Haslwanter, Michael Bahn, Ulrike Tappeiner, and Alexander Cernusca (2008). "Seasonal and inter-annual variability of the net ecosystem CO2 exchange of a temperate mountain grassland: Effects of weather and management". *Journal of Geophysical Research: Atmospheres* 113.D8.

Wolf, Sebastian, Trevor F Keenan, Joshua B Fisher, Dennis D Baldocchi, Ankur R Desai, Andrew D Richardson, Russell L Scott, Beverly E Law, Marcy E Litvak, Nathaniel A Brunsell, et al. (2016). "Warm spring reduced carbon cycle impact of the 2012 US summer drought". *Proceedings of the National Academy of Sciences* 113.21, pp. 5880–5885.

Yamazaki, Takeshi, Kyoko Kato, Tamaki Ito, Taro Nakai, Kazuho Matsumoto, Naoko Miki, Hotaek Park, and Takeshi Ohta (2013). "A common stomatal parameter set used to simulate the energy and water balance over boreal and temperate forests". *Journal of the Meteorological Society of Japan. Ser. II* 91.3, pp. 273–285.

Yu, Gui-Rui, Xue-Fa Wen, Xiao-Min Sun, Bertrand D Tanner, Xuhui Lee, and Jia-Yi Chen (2006). "Overview of ChinaFLUX and evaluation of its eddy covariance measurement". *Agricultural and Forest Meteorology* 137.3-4, pp. 125–137.

Zhang, Jun-Hui, Shi-Jie Han, and Gui-Rui Yu (2006). "Seasonal variation in carbon dioxide exchange over a 200-year-old Chinese broad-leaved Korean pine mixed forest". *Agricultural and Forest Meteorology* 137.3-4, pp. 150–165.

Zhao, Maosheng and Steven W Running (2010). "Drought-induced reduction in global terrestrial net primary production from 2000 through 2009". *Science* 329.5994, pp. 940–943.

Zimmermann, Frank, Kirsten Plessow, Ronald Queck, Christian Bernhofer, and Jörg Matschullat (2006). "Atmospheric N-and S-fluxes to a spruce forest—Comparison of inferential modelling and the throughfall method". *Atmospheric Environment* 40.25, pp. 4782–4796.

Zomer, Robert J., Antonio Trabucco, Deborah A. Bossio, and Louis V. Verchot (2008). "Climate change mitigation: A spatial analysis of global land suitability for clean development mechanism afforestation and reforestation". *Agriculture, ecosystems & environment* 126.1-2, pp. 67–80.

## Bayesian Modeling

We used Bayesian estimation to fit linear mixed effects models relating GPP to $NIR_V$. For the sake of simplicity, we modeled annual or monthly GPP as a linear function of $NIR_V$, and explored a variety of model structures allowing both slopes and intercepts to differ by land cover class or leaf habit, with random site-level effects. Preliminary model selection suggested that site-level random slope and intercept terms were not needed for the annual model, but were needed for monthly model. For the annual model, we explored a variety of fixed effects structures, as well as a number of variance functions (for residual variation and site-level intercepts). See Table S1 for list of annual models explored and their associated Deviance Information Criteria scores (DIC). All error functions assumed normally distributed errors and similar functional forms for residual error and site random intercepts, but with residual errors being a function of observed annual $NIR_V$ and site random intercepts a function of site mean annual $NIR_V$. Considerably more complicated model formulations (e.g. estimating retrieval error in $NIR_V$ by treating true $NIR_V$ as a latent variable, incorporating information on error in fluxtower GPP estimates) can be implemented in this modeling framework, though we present the simplest defensible case for the sake of illustration and intuitive upscaling. We produced global annual estimates of GPP using the posterior distribution of the best annual $NIR_V$ model (bolded in Table S1). We excluded pixels with a landcover classification of "barren". We have posted the GPP calibration code to www.github.com/badgley/nirv-global.

We used Markov chain Monte Carlo simulations (MCMC) implemented in JAGS to sample the joint posterior distribution of fitted models, with diffuse priors for all parameters Plummer, 2003. We ran three parallel MCMC chains, ensuring chain convergence and thinning chains to remove within-chain autocorrelation to produce 1000 nearly independent draws from the posterior. We report median estimates and 95% credible intervals for model parameters, and upscaled GPP estimates, based on the joint posterior distribution of the best model.

## Cross Validation

We took the added step of refitting the full Bayesian model using 10-fold cross validation to ensure the robustness of model specification. First, we stratified our data by both site and ecosystem type, assigning 10% of deciduous, evergreen, and crop sites (including all site years for those sites) to each fold. We then fit the model, withholding a single fold, and analyzed the variation of individual

model parameters. The mean value of each cross-validated model parameter fell well within the 95% credible interval of the full model posterior distribution for that parameter, indicating the robustness of the full model to changes in training data (Figure S6).

## Model Comparison by Modified AIC

We conducted a *post hoc* AIC analysis of BESS, FLUXCOM, and $NIR_V$-derirved GPP estimates, calculating AIC as: $n \cdot log(MSE) + 2 \cdot p$, where n is the number of site years, MSE is the mean square error of modeled versus observed GPP, and p is the number of fit parameters. We only included site-years in the analysis that were available across all three products. For the comparison products, MSE were calculated using data provided directly from the authors of FLUXCOM and BESS, and number of parameters was estimated extremely conservatively (e.g. assuming only a single parameter per input variable for the FLUXCOM machine learning-base product).

## Open Source Software

### Python

All analyses, with the exception of the Bayesian modeling, were performed using the Python programming language. We processed netCDF files and tabular data using xarray Hoyer et al., 2017, pandas McKinney et al., 2010, and numpy Walt et al., 2011. We used matplotlib Hunter, 2007 and seaborn Waskom et al., 2014 for visualization, and Jupyter notebooks for organizing analyses Kluyver et al., 2016.

### R

We ran all Bayesian modeling in the R programming environment Team, 2014, making use of the "r2jags" package Su et al., 2015 to interface with JAGS, a Bayesian modeling software package Plummer, 2013.

| Model Structure | Variance Structure | Fixed Params | DIC |
|---|---|---|---|
| GPP = intercept + $NIR_V$:leaf habit | $a$ | 4 | 7142.393 |
| GPP = intercept + $NIR_V$:leaf habit | $a + b \cdot NIR_V$ | 4 | 7134.997 |
| GPP = intercept + $NIR_V$:leaf habit | $a + e^{zNIR_V \cdot b}$ | 4 | 7146.137 |
| GPP = intercept + $NIR_V$:leaf habit | $a + b \cdot e^{zNIR_V}$ | 4 | 7150.204 |
| GPP = intercept + $NIR_V$:leaf habit | $a + NIR_V^b$ | 4 | 7150.299 |
| **GPP = intercept + $NIR_V$:leaf habit** | $NIR_V^b$ | **4** | **7104.392** |
| GPP = intercept + $NIR_V$:leaf habit | $a + b * NIR_V^2$ | 4 | 7127.383 |
| GPP = intercept:leaf habit + slope:leaf habit | $NIR_V^b$ | 6 | 7106.333 |
| GPP = intercept:land cover + slope:land cover | $NIR_V^b$ | 22 | 7106.601 |
| GPP = intercept + slope:land cover | $NIR_V^b$ | 12 | 7111.44 |

**Table S1.** Potential annual models tested, including various fixed structures and various variance formulations. Variance functions were fit for the standard deviation of both the residual error and the site-level random intercept, where $NIR_V$ is annual observed $NIR_V$ for the residual error and the site mean annual $NIR_V$ for the site random intercept. "z$NIR_V$" indicates that $NIR_V$ values were z-score standardized.

| Model | RMSE | Marginal $R^2$ |
|---|---|---|
| $NIR_V$ | 363.9 | 0.68 |
| NDVI | 410.3 | 0.59 |
| fPAR | 443.4 | 0.52 |
| $PAR \cdot NIR_V$ | 454.1 | 0.50 |

**Table S2.** Performance of alternative models, testing the suitability of NDVI, fPAR, and PAR for predicting GPP. $NIR_V$ has the best performance over all metrics.

| Model | RMSE | Marginal R2 | DIC |
|---|---|---|---|
| NIRv | 362.39 | 0.68 | 6769.24 |
| NIRv + Precip | 350.14 | 0.70 | 6774.04 |
| NIRv + Temp | 363.23 | 0.64 | 6775.41 |
| NIRv + VPD | 355.86 | 0.69 | 6775.51 |
| NIRv + PAR | 360.87 | 0.68 | 6773.15 |
| NIRv + All Met | 336.77 | 0.72 | 6776.86 |

**Table S3.** Performance of alternative Bayesian models that include meteorological variables (excluding three site-years without meteorological data). RMSE and $R^2$ of meteorological models typically outperforms the baseline $NIR_V$ model. However, the $NIR_V$ model has the lowest DIC, indicating the improved performance from including meteorological information comes at the expense of model generality and possible overfitting.

| | $NIR_V$ | | BESS | | FLUXCOM | |
|---|---|---|---|---|---|---|
| | GPP (Pg C $y^{-1}$) | Fraction (%) | GPP (Pg C $y^{-1}$) | Fraction (%) | GPP (Pg C $y^{-1}$) | Fraction (%) |
| Evergreen Broadleaf Forest | 46.74 | 31.70 | 40.18 | 33.66 | 40.48 | 34.21 |
| Mixed forest | 16.28 | 11.04 | 10.61 | 8.89 | 11.24 | 9.50 |
| Woody savannas | 15.00 | 10.17 | 15.21 | 12.74 | 14.12 | 11.94 |
| Savannas | 14.79 | 10.03 | 13.08 | 10.96 | 13.00 | 10.99 |
| Croplands | 13.82 | 9.38 | 10.42 | 8.73 | 10.48 | 8.86 |
| Grasslands | 12.11 | 8.21 | 9.25 | 7.75 | 7.84 | 6.63 |
| Open shrublands | 10.89 | 7.39 | 6.01 | 5.04 | 6.23 | 5.27 |
| Cropland Mosaic | 9.74 | 6.61 | 8.98 | 7.52 | 8.64 | 7.30 |
| Evergreen Needleleaf Forest | 4.12 | 2.80 | 2.69 | 2.26 | 2.87 | 2.42 |
| Other | 1.97 | 1.34 | 1.69 | 1.41 | 1.55 | 1.31 |
| Deciduous Broadleaf Forest | 1.96 | 1.33 | 1.24 | 1.04 | 1.87 | 1.58 |

**Table S4.** Per biome distribution GPP for $NIR_V$, BESS, and FLUXCOM global GPP products.

| Site | Latitude | Longitude | Years | Reference |
|---|---|---|---|---|
| AR-Vir | -28.2395 | -56.1886 | 2009–2012 | Posse et al., 2016 |
| AT-Neu | 47.1167 | 11.3175 | 2002–2012 | Wohlfahrt et al., 2008 |
| AU-ASM | -22.283 | 133.249 | 2010–2013 | Eamus et al., 2013 |
| AU-Ade | -13.0769 | 131.1178 | 2007–2009 | Beringer et al., 2011 |
| AU-Cpr | -34.0021 | 140.5891 | 2010–2013 | Karan et al., 2016 |
| AU-Cum | -33.6133 | 150.7225 | 2012–2013 | Karan et al., 2016 |
| AU-DaP | -14.0633 | 131.3181 | 2008–2013 | Beringer et al., 2011 |
| AU-DaS | -14.1593 | 131.3881 | 2008–2013 | Beringer et al., 2011 |
| AU-Dry | -15.2588 | 132.3706 | 2008–2013 | Beringer et al., 2011 |
| AU-Emr | -23.8587 | 148.4746 | 2011–2013 | Schroder, 2014 |
| AU-Fog | -12.5452 | 131.3072 | 2006–2008 | Beringer et al., 2011 |
| AU-GWW | -30.1913 | 120.6541 | 2013–2014 | Prober et al., 2012 |
| AU-RDF | -14.5636 | 132.4776 | 2011–2013 | Beringer et al., 2011 |
| AU-Rig | -36.6499 | 145.5759 | 2011–2013 | Beringer et al., 2011 |
| AU-Tum | -35.6566 | 148.1517 | 2001–2013 | Leuning et al., 2005 |
| AU-Whr | -36.6732 | 145.0294 | 2011–2013 | Karan et al., 2016 |
| BE-Bra | 51.3092 | 4.5206 | 2000–2013 | Carrara et al., 2003 |
| BE-Lon | 50.5516 | 4.7461 | 2004–2014 | Moureaux et al., 2006 |
| BE-Vie | 50.3051 | 5.9981 | 2000–2014 | Aubinet et al., 2001 |
| BR-Sa3 | -3.018 | -54.9714 | 2000–2004 | Miller et al., 2004 |
| CA-NS1 | 55.8792 | -98.4839 | 2002–2005 | Goulden et al., 2006 |
| CA-NS2 | 55.9058 | -98.5247 | 2001-2005 | Goulden et al., 2006 |
| CA-NS3 | 55.9117 | -98.3822 | 2001–2005 | Goulden et al., 2006 |
| CA-NS4 | 55.9117 | -98.3822 | 2002–2005 | Goulden et al., 2006 |
| CA-NS5 | 55.8631 | -98.485 | 2001–2005 | Goulden et al., 2006 |
| CA-NS6 | 55.9167 | -98.9644 | 2001–2005 | Goulden et al., 2006 |
| CA-NS7 | 56.6358 | -99.9483 | 2002–2005 | Goulden et al., 2006 |
| CA-Qfo | 49.6925 | -74.3421 | 2003–2010 | Bergeron et al., 2007 |
| CH-Cha | 47.2102 | 8.4104 | 2006–2012 | Eugster et al., 2006 |

| | | | | |
|---|---|---|---|---|
| CH-Fru | 47.1158 | 8.5378 | 2006–2012 | Eugster et al., 2006 |
| CH-Oe1 | 47.2858 | 7.7319 | 2002–2008 | Ammann et al., 2007 |
| CN-Cha | 42.4025 | 128.0958 | 2003–2005 | Zhang et al., 2006 |
| CN-Cng | 44.5934 | 123.5092 | 2007–2010 | Dong et al., 2011 |
| CN-Dan | 30.4978 | 91.0664 | 2004–2005 | Yu et al., 2006 |
| CN-Din | 23.1733 | 112.5361 | 2003–2005 | Yu et al., 2006 |
| CN-Du2 | 42.0467 | 116.2836 | 2006–2008 | Chen et al., 2009 |
| CN-Ha2 | 37.6086 | 101.3269 | 2003–2005 | Fu et al., 2006 |
| CN-HaM | 37.37 | 101.18 | 2002–2004 | Kato et al., 2006 |
| CN-Qia | 26.7414 | 115.0581 | 2003–2005 | Yu et al., 2006 |
| CN-Sw2 | 41.7902 | 111.8971 | 2010–2012 | Shao et al., 2013 |
| DE-Akm | 53.8662 | 13.6834 | 2009–2014 | http://www.fluxdata.org:8080/sitepages/siteInfo.aspx?DE-Akm |
| DE-Gri | 50.9495 | 13.5125 | 2004–2014 | Gilmanov et al., 2007 |
| DE-Hai | 51.0792 | 10.453 | 2000–2012 | Knohl et al., 2003 |
| DE-Kli | 50.8929 | 13.5225 | 2004–2014 | Ceschia et al., 2010 |
| DE-Obe | 50.7836 | 13.7196 | 2008–2014 | Zimmermann et al., 2006 |
| DE-RuS | 50.8659 | 6.4472 | 2011–2014 | Mauder et al., 2013 |
| DE-Sfn | 47.8064 | 11.3275 | 2012-2014 | Hommeltenberg et al., 2014 |
| DE-Spw | 51.8923 | 14.0337 | 2010–2014 | http://www.fluxdata.org:8080/sitepages/siteInfo.aspx?DE-spw |
| DE-Tha | 50.9636 | 13.5669 | 2000–2014 | GrüNwald et al., 2007 |
| DK-Sor | 55.4859 | 11.6446 | 2000–2012 | Pilegaard et al., 2001 |
| ES-LgS | 37.0979 | -2.9658 | 2007–2009 | Reverter et al., 2010 |
| FI-Hyy | 61.8475 | 24.295 | 2000–2014 | Vesala et al., 2005 |
| FR-Gri | 48.8442 | 1.9519 | 2004–2013 | Loubet et al., 2011 |
| FR-Fon | 48.4764 | 2.7801 | 2005-2014 | Delpierre et al., 2016 |
| FR-Pue | 43.7414 | 3.5958 | 2000–2013 | Rambal et al., 2004 |
| GF-Guy | 5.2788 | -52.9249 | 2004–2012 | Bonal et al., 2008 |
| IT-BCi | 40.5238 | 14.9574 | 2004-2014 | Vitale et al., 2016 |
| IT-CA1 | 42.3804 | 12.0266 | 2011–2013 | Sabbatini et al., 2016 |
| IT-CA2 | 42.3772 | 12.026 | 2011–2013 | Sabbatini et al., 2016 |
| IT-CA3 | 42.38 | 12.0222 | 2011–2013 | Sabbatini et al., 2016 |

| | | | | |
|---|---|---|---|---|
| IT-Cp2 | 41.7043 | 12.3573 | 2012–2013 | Fares et al., 2015 |
| IT-Isp | 45.8126 | 8.6336 | 2013–2014 | Ferréa et al., 2012 |
| IT-Lav | 45.9562 | 11.2813 | 2003–2012 | Cescatti et al., 2003 |
| IT-Noe | 40.6061 | 8.1515 | 2004–2012 | Spano et al., 2005 |
| IT-PT1 | 45.2009 | 9.061 | 2002–2004 | Migliavacca et al., 2009 |
| IT-Ren | 46.5869 | 11.4337 | 2000–2013 | Marcolla et al., 2005 |
| IT-Ro1 | 42.4081 | 11.93 | 2000–2008 | Rey et al., 2002 |
| IT-Ro2 | 42.3903 | 11.9209 | 2002–2012 | Tedeschi et al., 2006 |
| IT-SR2 | 43.732 | 10.291 | 2013–2014 | Matteucci et al., 2015 |
| IT-SRo | 43.7279 | 10.2844 | 2000–2012 | Matteucci et al., 2015 |
| IT-Tor | 45.8444 | 7.5781 | 2008–2013 | Galvagno et al., 2013 |
| JP-MBF | 44.3869 | 142.3186 | 2003–2005 | Yamazaki et al., 2013 |
| JP-SMF | 35.2617 | 137.0788 | 2002–2006 | Yamazaki et al., 2013 |
| NL-Hor | 52.2404 | 5.0713 | 2004–2011 | Van der Molen et al., 2004 |
| NL-Loo | 52.1666 | 5.7436 | 1996–2013 | Dolman et al., 2002 |
| RU-Fyo | 56.4615 | 32.9221 | 2000–2013 | Kurbatova et al., 2008 |
| SD-Dem | 13.2829 | 30.4783 | 2005–2009 | Sjöström et al., 2009 |
| US-AR1 | 36.4267 | -99.42 | 2009–2012 | Billesbach et al., 2016 |
| US-AR2 | 36.6358 | -99.5975 | 2009–2012 | Billesbach et al., 2016 |
| US-ARM | 36.6058 | -97.4888 | 2003–2012 | Fischer et al., 2007 |
| US-Blo | 38.8953 | -120.633 | 2000–2007 | Goldstein et al., 2000 |
| US-Ha1 | 42.5378 | -72.1715 | 2000–2012 | Urbanski et al., 2007 |
| US-Los | 46.0827 | -89.9792 | 2000–2014 | Sulman et al., 2009 |
| US-MMS | 39.3232 | -86.4131 | 2000–2014 | Schmid et al., 2000 |
| US-Me2 | 44.4523 | -121.5574 | 2002-2014 | Law et al., 2006 |
| US-Me6 | 44.3233 | -121.608 | 2010–2012 | Ruehr et al., 2012 |
| US-Myb | 38.0498 | -121.765 | 2011–2014 | Sturtevant et al., 2016 |
| US-Ne1 | 41.1651 | -96.4766 | 2001–2013 | Verma et al., 2005 |
| US-Ne2 | 41.1649 | -96.4701 | 2001–2013 | Verma et al., 2005 |
| US-Ne3 | 41.1797 | -96.4397 | 2001–2013 | Verma et al., 2005 |
| US-NR1 | 40.0329 | -105.5464 | 1998-2014 | Monson et al., 2002 |

| | | | | |
|---|---|---|---|---|
| US-PFa | 45.9459 | -90.2723 | 1995-2014 | Desai et al., 2015 |
| US-SRG | 31.7894 | -110.8277 | 2008-2014 | Scott et al., 2015 |
| US-SRM | 31.8214 | -110.866 | 2004–2014 | Scott, 2010 |
| US-Syv | 46.242 | -89.3477 | 2001–2014 | Desai et al., 2005 |
| US-Ton | 38.4316 | -120.966 | 2001–2014 | Baldocchi et al., 2004 |
| US-Twt | 38.1087 | -121.6530 | 2009-2014 | Hatala et al., 2012 |
| US-UMB | 45.5598 | -84.7138 | 2000-2014 | Rothstein et al., 2000 |
| US-UMd | 45.5625 | -84.6975 | 2007–2014 | Gough et al., 2013 |
| US-Var | 38.4133 | -120.951 | 2000–2014 | Ma et al., 2007 |
| US-WCr | 45.8059 | -90.0799 | 2000–2014 | Cook et al., 2004 |
| US-Whs | 31.7438 | -110.052 | 2007–2014 | Scott, 2010 |
| US-Wkg | 31.7365 | -109.942 | 2004–2014 | Scott, 2016 |
| ZA-Kru | -25.0197 | 31.4969 | 2000–2010 | Scholes et al., 2001 |
| ZM-Mon | -15.4378 | 23.2528 | 2007–2009 | Scanlon et al., 2004 |

**Table S5.** The FLUXNET2015 sites used in this study.

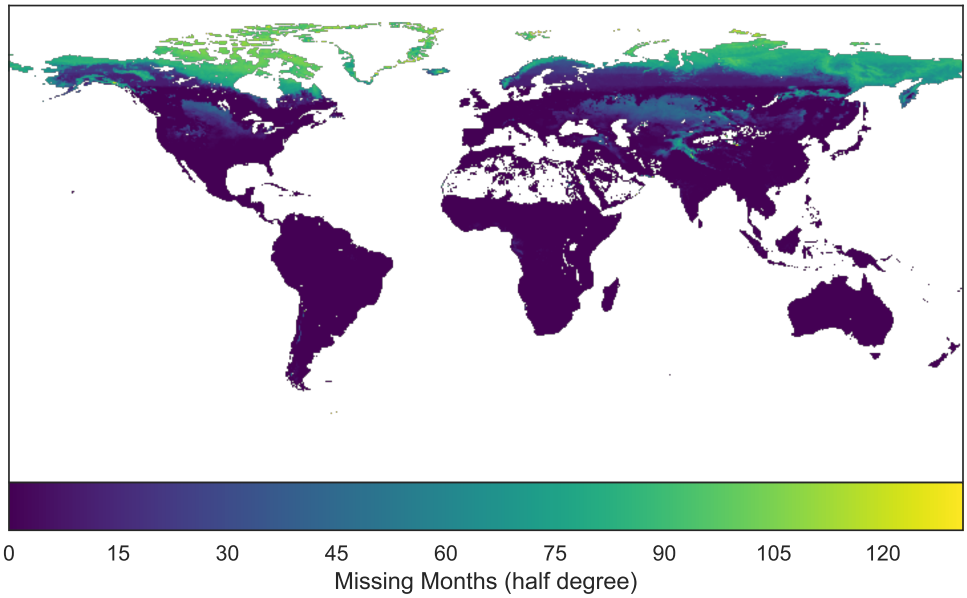


**Figure S1.** Number of months with valid $NIR_V$ measurements from the MCD43 reflectance data product.

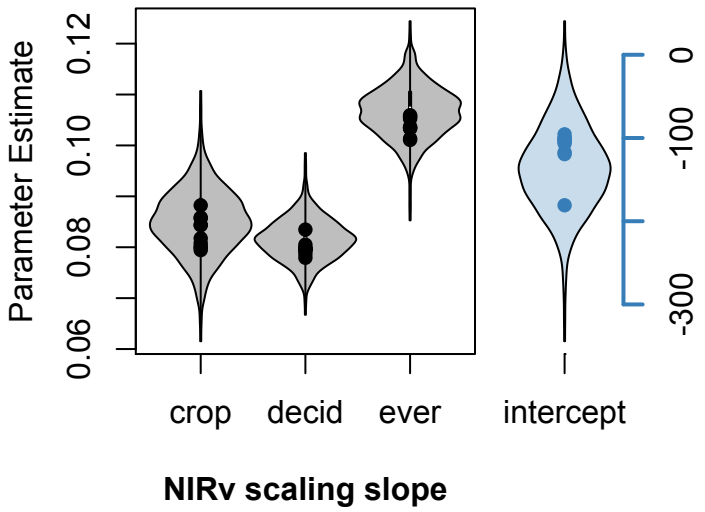


**Figure S2.** Comparison of full model posterior parameter estimates versus 10-fold cross validation parameter estimates. Violin plots show the posterior densities for parameter estimates (three scaling slopes and single intercept) from the model trained with all data. Points show the mean parameter estimates for cross validation models after holding each of 10 folds out of model training. Folds were stratified by site and ecosystem-type. All cross validation mean parameter estimates fall within the 95% credible intervals of the full model.

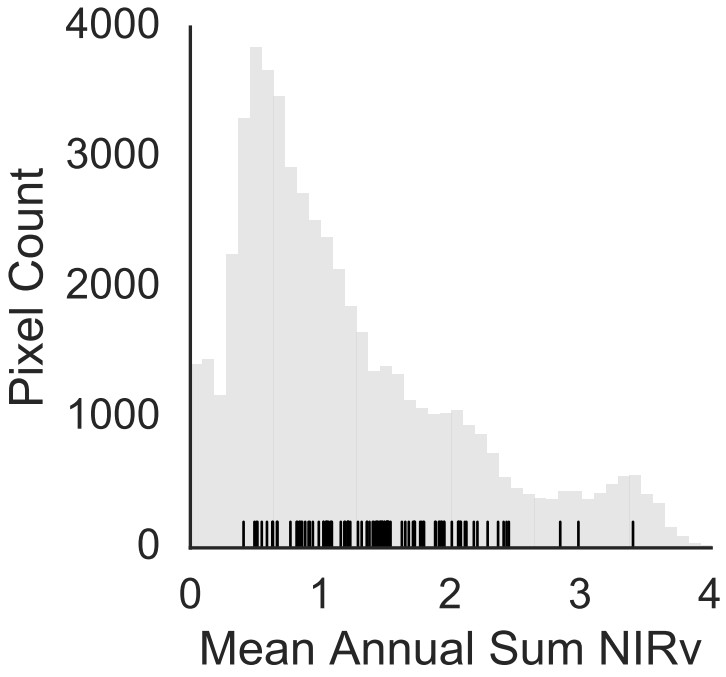


**Figure S3.** The global distribution of mean sum $NIR_V$ at half-degree resolution (grey bars), with FLUXNET2015 calibration sites shown in black hatching.

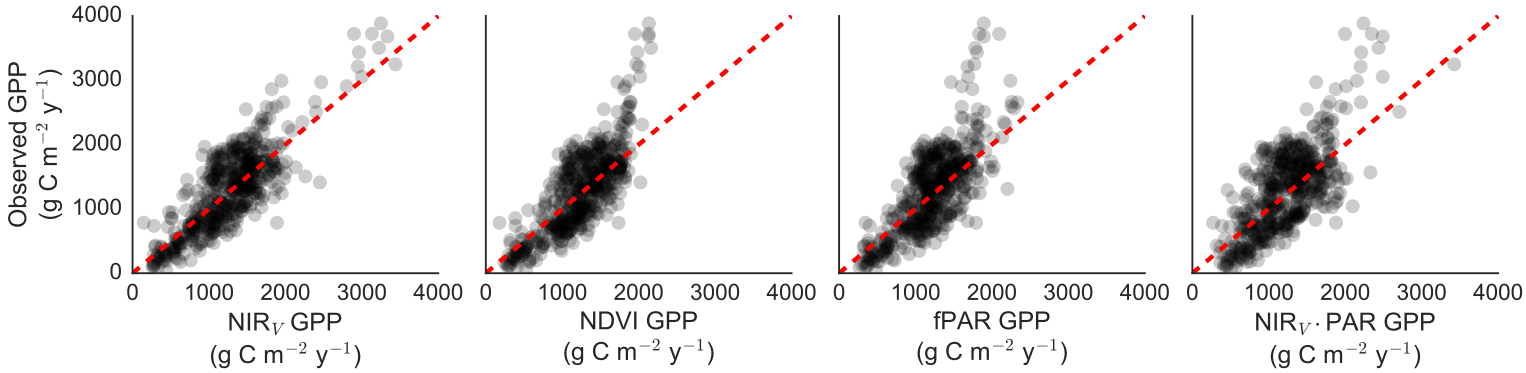


**Figure S4.** Predicted GPP values plotted against annual observed GPP at 105 flux sites for A) $\mathrm{NIR_V}$, B) NDVI, C) fPAR, and D) $PAR \cdot NIR_V$.

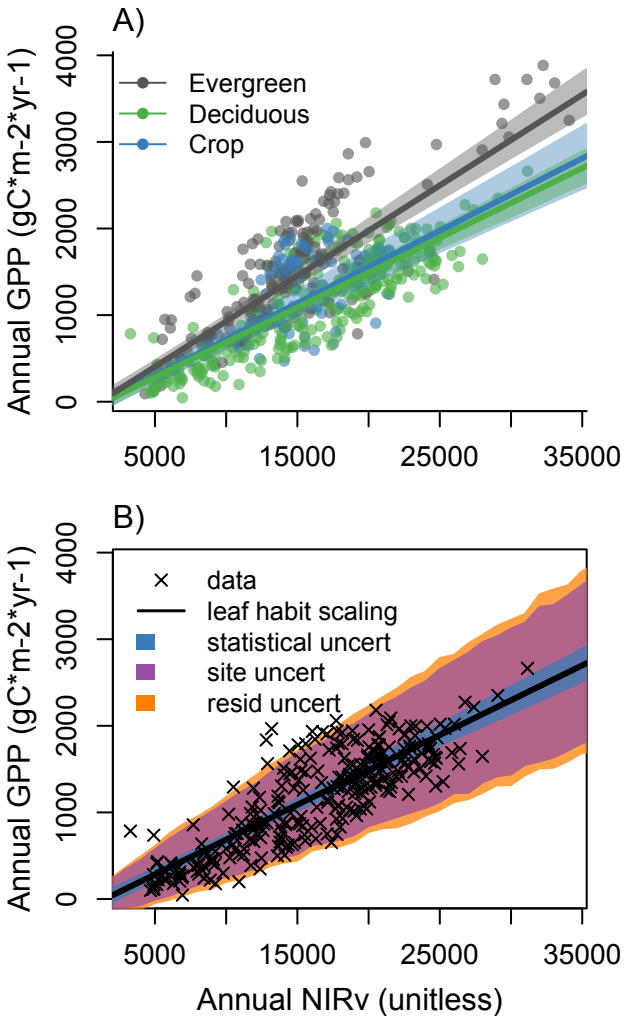


**Figure S5.** Depiction of A) the final model formulation and B) the structure of model uncertainties. Each leaf habit shared an intercept, but had slightly different $NIR_V$ to GPP slope. Errors increased exponentially with observed $NIR_V$, with site-level uncertainty having the largest relative contribution to total per pixel error.

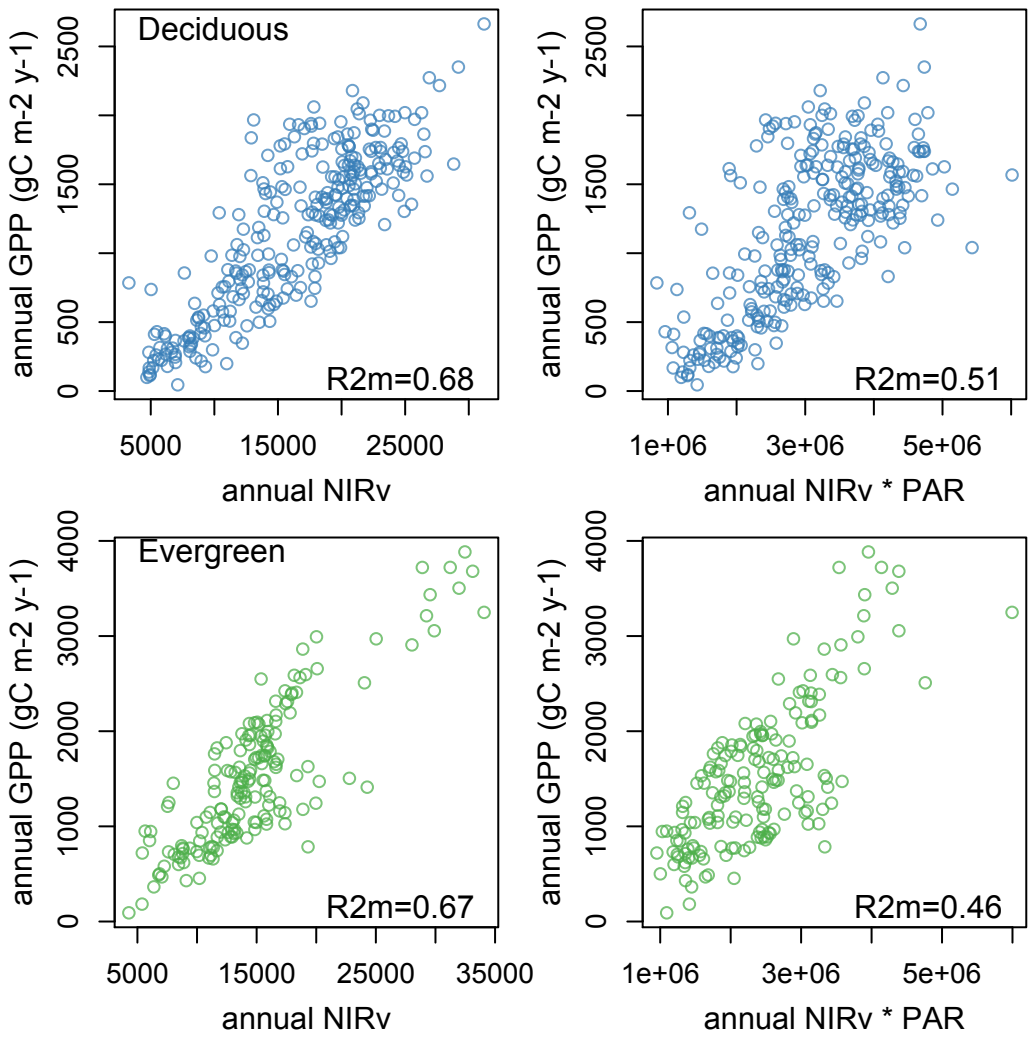


**Figure S6.** A direct comparison of NIRv and NIRv*PAR for the annual calibration data. Including PAR does not improve model performance.

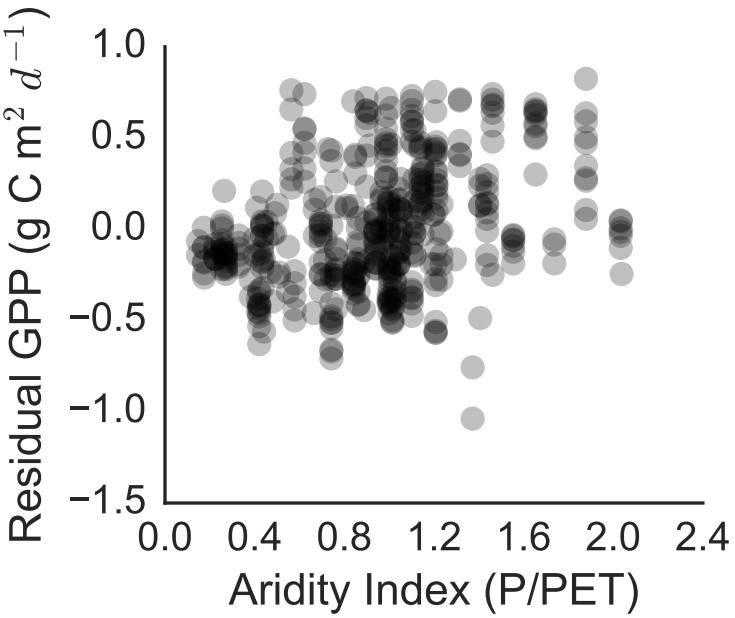


**Figure S7.** Residual GPP from NIRv-based model plotted against calibration site aridity index (P/PET). PET data were taken from: https://cgiarcsi.community/data/global-aridity-and-pet-database/ (Zomer et al., 2008)

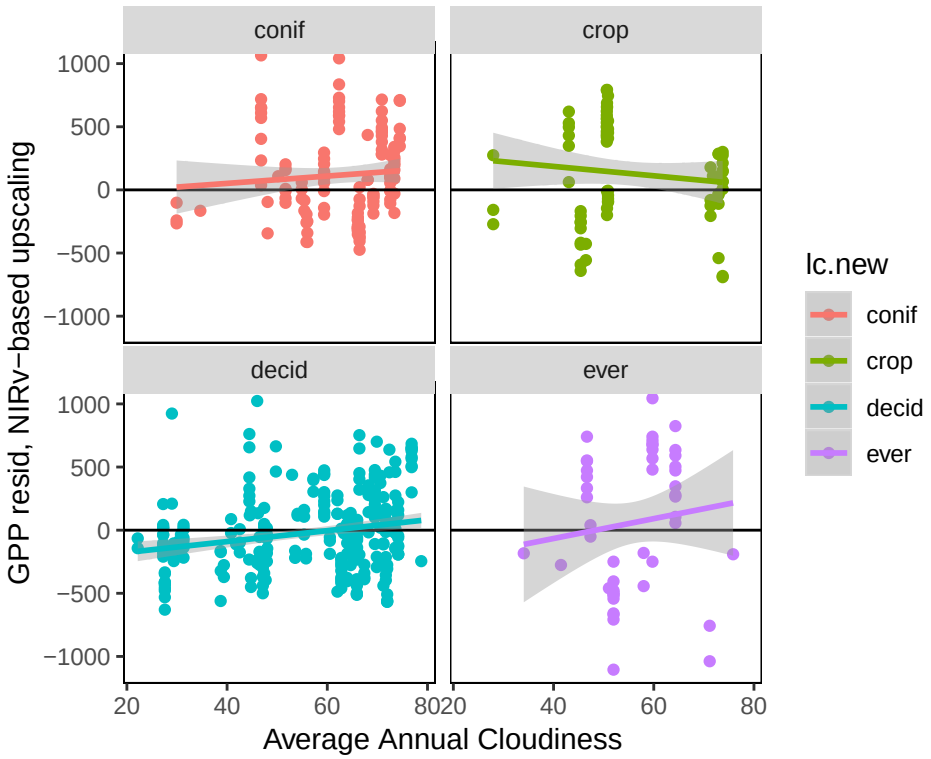


**Figure S8.** There was no significant relationship between model residual GPP and site average annual cloudiness. Cloud data taken from Wilson et al. (2016).

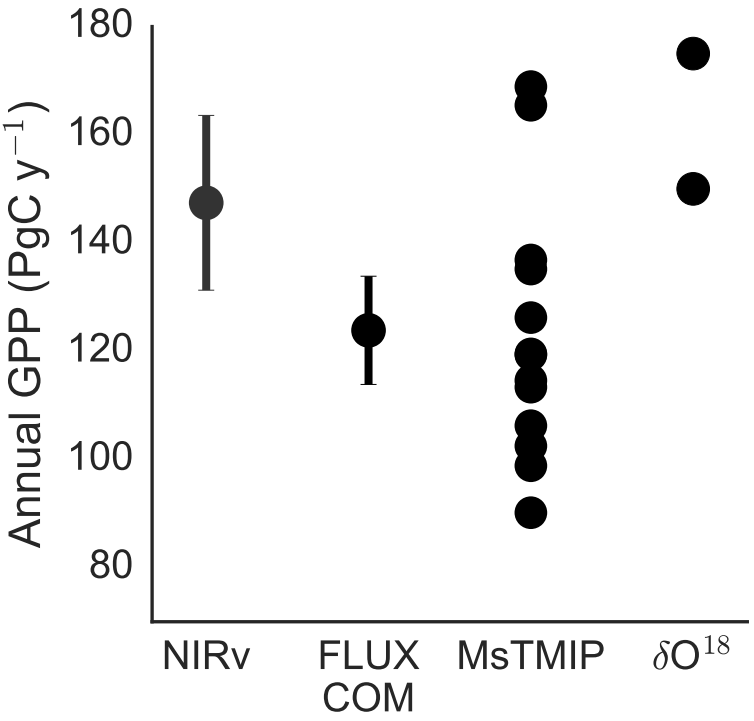


**Figure S9.** Comparison of $NIR_V$, FLUXCOM, MsTMIP, and oxygen isotopic constraint on GPP. MsTMIP data downloaded from https://daac.ornl.gov/cgi-bin/dsviewer.pl?ds_id=1225.

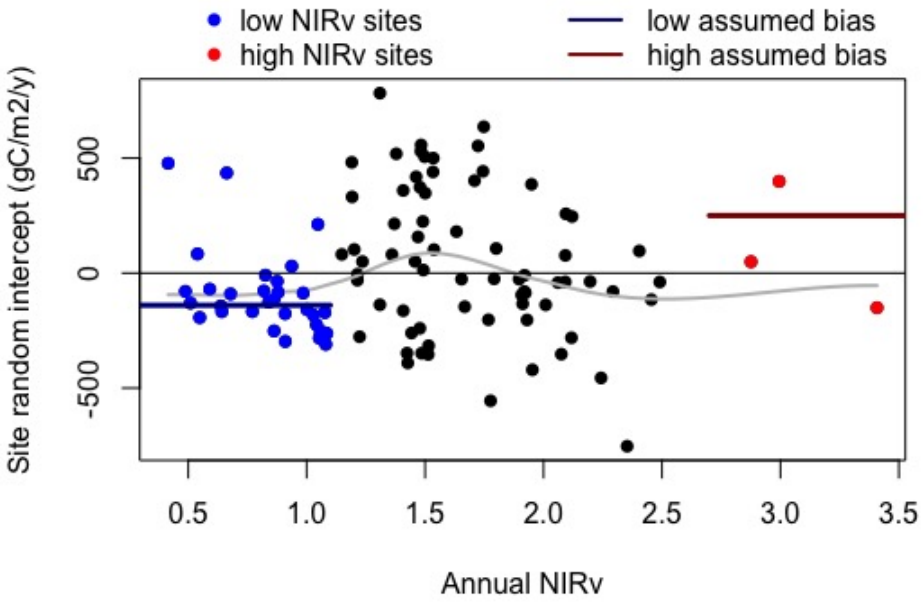


**Figure S10.** Site random intercept plotted against site annual $NIR_V$ shows little evidence of systematic bias. Assuming a worst case scenario of bias (red, 0.27 kg C $m^{-2}$ $y^{-1}$ of underestimation for high NIRv pixels; blue, 0.14 kg C $m^{-2}$ $y^{-1}$ of overestimation for low NIRv pixel), neither maximum credible bias would affect our global estimate of GPP by more than 10%.

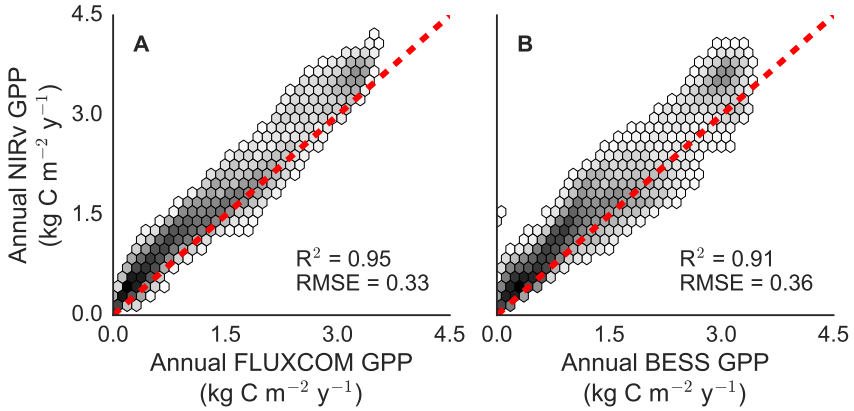


**Figure S11.** Upscaled $NIR_V$-based estimates of annual GPP are linear with both A) FLUXCOM and B) BESS GPP estimates. $NIR_V$-based estimates tend to be slightly higher than both FLUXCOM and BESS, though $NIR_V$ has low a RMSE relative to both products. $NIR_V$-based GPP estimate shown as the median case of 1000 nearly independent upscalings, see Methods.

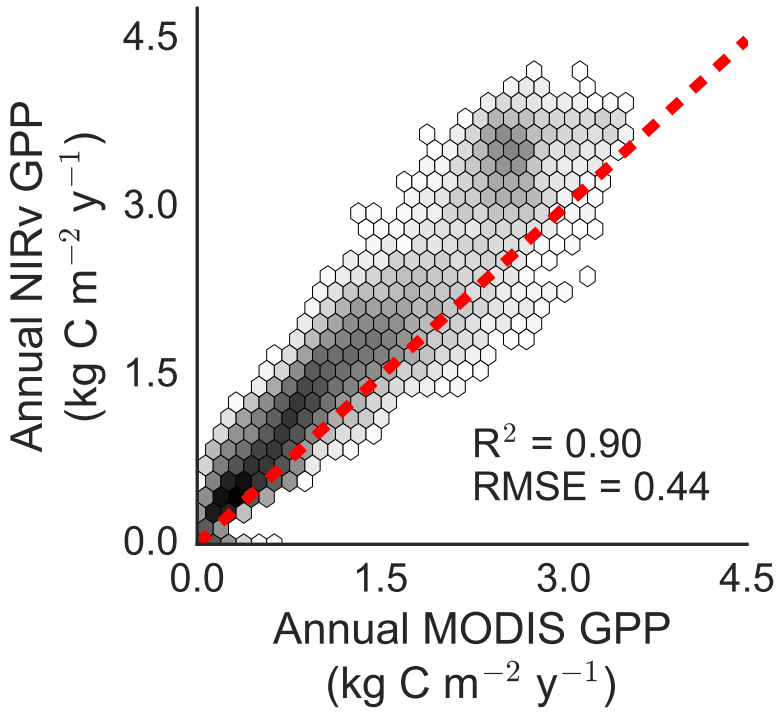


**Figure S12.** Per-pixel comparison of NIRv-derived estimates of GPP and the MODIS GPP product, spanning 2003 to 2015.

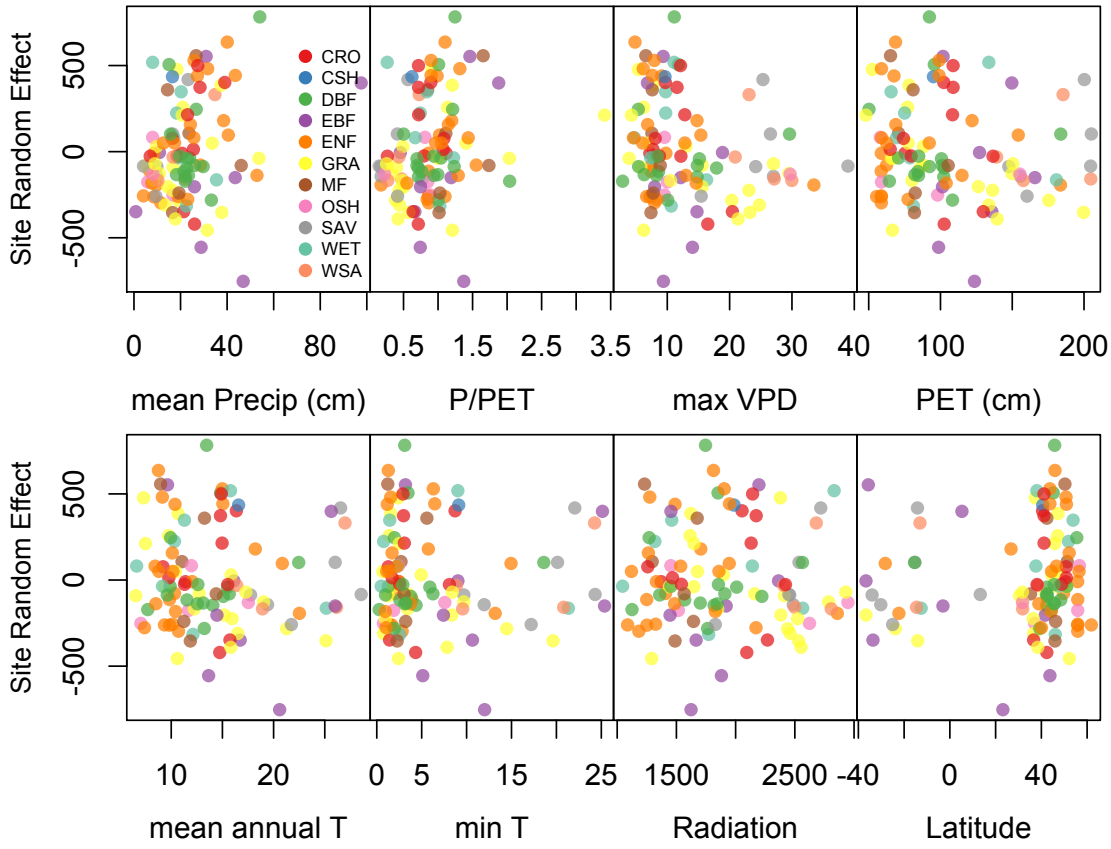


**Figure S13.** Site-level random intercepts plotted against various, site-level meteorological data show no coherent patterns, indicating that site-to-site uncertainty is a product of uncertainties in $NIR_V$ and GPP used for model calibrations, as opposed to environmental factors not included in the model.

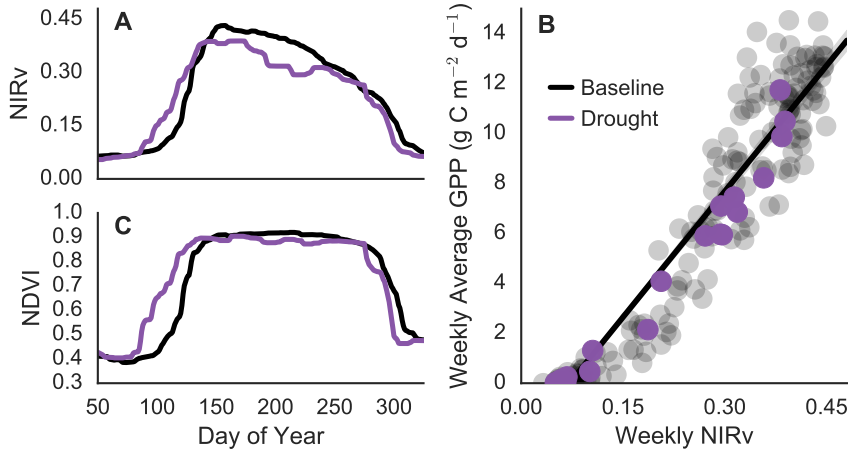


**Figure S14.** During the 2012 North American drought, A) $NIR_V$ shows distinctive early spring shift and suppression throughout the summer months when compared against non-drought (baseline) years. B) Despite these phenological changes, $NIR_V$ tightly tracks GPP. C) NDVI during the dourght shows a spring shift, but little difference in peak summer values.